EFFECTS OF A BOREHOLE ENVIRONMENT AND RESIDUAL HYDROCARBON ON STONELEY WAVE AMPLITUDE AND REFLECTIVITY

Guo Tao and C. H. Cheng

Earth Resources Laboratory
Department of Earth, Atmospheric, and Planetary Sciences
Massachusetts Institute of Technology
Cambridge, MA 02139

ABSTRACT

In recent years, borehole Stoneley wave amplitude and reflectivity have been used for estimating formation permeability based on the strong correlation between Stoneley wave attenuation, reflectivity and formation fluid conductivity. There are other factors, however, that may cause substantial Stoneley attenuation and reflection in a borehole environment. To make better use of Stoneley measurements for formation permeability estimation, it is desirable to identify and quantify those causes of Stoneley attenuation and reflection that do not directly result from formation permeability. In this study, a simplified Biot-Rosenbaum model developed by Tang *et al.* (1991) is adopted to systematically model Stoneley attenuation and reflection in various borehole environments and formation configurations. By changing pore fluid, formation porosity, lithology, bed boundaries and thickness in the modeling, the sensitivity of Stoneley wave propagation to these conditions are quantitatively assessed. It is found that the presence of a light hydrocarbon in the formation, especially a natural gas residual in the immediate vicinity of the borehole wall, even with only 5% contained in pore fluid, may also cause substantial Stoneley attenuation and reflection. This phenomenon, on the other hand, can be used to evaluate a nonfractured, low permeability gas reservoir when combined with shear wave velocity data. For the full gas-saturated zone, Stoneley wave reflection may be observed even when the permeability is as low as a few milliDarcies. Compared to the effects of pore fluid, the effects due to lithology contrasts at the boundaries and the changes of nonfracture porosity are insignificant in the cases studied here. For a residual gas-bearing zone of moderate permeability, Stoneley wave attenuation and reflection may be observed if the zone is thicker than 0.5 meter.

INTRODUCTION

Borehole Stoneley wave amplitude has been known to be very sensitive to formation permeability (Paillet, 1980; Williams *et al.*, 1990). Theoretical models based on Biot (1962) theory have been developed (Rosenbaum, 1974; Schmitt *et al.*, 1988) and have been validated by laboratory measurements (Winkler *et al.*, 1989). These models have also been used to formulate inversion procedures for estimating permeability from Stoneley wave data (Burns, 1990; Cheng and Cheng, 1991). Recently, Tang *et al.* (1991) developed a simplified Biot model for borehole Stoneley wave propagation. This model yields results that are consistent with full Biot theory, but the formulation and computation are simplified. More recently, this model has been expanded to include tool effects (Tang and Cheng, 1993) and the influence of borehole enlargement (Tezuka *et al.*, 1994; Tang *et al.*, 1995). Tang and Cheng (1994) further developed a fast inversion procedure for estimating permeability from Stoneley wave data based on the model. Zhao *et al.* (1994) used this method to investigate the effects of formation permeability heterogeneities on Stoneley wave propagation and developed a technique, in conjunction with a variable permeability model, to successfully model the nonsymmetric patterns of Stoneley wave attenuation and reflection at the top and bottom of the fracture zone; it was not possible to explain the phenomena with a homogeneous permeable zone model.

Although these researchers have studied and modeled Stoneley wave attenuation and reflection due to fractured and permeable zones with homogeneous or heterogeneous permeability, to avoid misinterpretation of Stoneley energy propagation in a borehole surrounded by gas-bearing formation, it is desirable to identify and quantify those causes of Stoneley attenuation and reflection that do not directly result from formation permeability. Norris (1989) analyzed Stoneley wave attenuation and dispersion for the fully dynamic behavior and corroborated the findings of Rosenbaum (1974) and Schmitt *et al.* (1988) on the effects of permeability. He also concluded that Stoneley wave attenuation increases with permeability but depends critically on the pore saturant.

A crucial aspect of our study will be the construction of synthetic borehole seismograms as an aid in identifying various effects the borehole environment and the target zone have on Stoneley wave propagation. A numerical model for acoustic propagation in a borehole has been specifically chosen to allow the decomposition of waveforms into individual modes of propagation, i.e., the Stoneley or "tube" wave. Such a careful reconstruction of a waveform for various borehole environments and formation configurations should provide valuable insight into the physical effects associated with Stoneley wave energy propagation in a borehole.

In this study, we apply the numerical techniques developed by Tang *et al.* (1991, 1993) to model the effects of lithology, pore fluid, borehole size, formation porosity, thickness and bed boundaries on Stoneley attenuation and reflection. The effects of pore fluid, especially natural gas, in a permeable zone are of particular interest.

PRINCIPLES OF NUMERICAL MODELING

When the Stoneley wave propagates in a borehole across a permeable formation, the borehole wave excites three types of waves in the formation: compressional and shear waves ("fast" waves by Biot's definition) and the slow wave. The slow wave is primarily associated with the motion of pore fluid. In full Biot theory, the three waves are intimately coupled in their interaction with the borehole Stoneley wave (Rosenbaum, 1974). Therefore, the calculation is quite involved. In the simplified theory (Tang *et al.*, 1991), the interaction is decomposed into two parts. The first is the interaction of the Stoneley wave with the fast waves. (i.e., an equivalent elastic formation whose acoustic properties are those of the fluid-saturated rocks). The second is the interaction of the Stoneley wave with the slow wave. Because the frequency dependency of the dynamic fluid flow must be accounted for in the second interaction, the theory of dynamic permeability (Johnson *et al.*, 1987) has been employed to measure the amount of Stoneley wave energy that is carried away into the formation by the slow wave. In this way, the simplified model captures the frequency-dependent behavior of the slow wave and greatly simplifies the formulation and numerical computation involved.

During propagation across the permeable zone, the Stoneley wave attenuates its amplitude and also generates a reflected wave (Paillet and White, 1982; Hornby *et al.*, 1989). The reflection patterns, which we can easily see on the iso-offset waveform display, give good information about the fractures. However, Stoneley wave reflections occur not only because of the fractures and the permeable zone, but also because of lithology and borehole diameter changes (Paillet, 1980; Hardin *et al.*, 1987). In the cases of fractures and the permeable zone, pore saturating fluids have a significant effect on compressional wave velocity and attenuation (Toksöz *et al.*, 1976; Tao *et al.*, 1995) and Stoneley wave velocities and attenuation, (Schmitt, 1988; Norris, 1989) but an insignificant effect on shear wave velocities and attenuation.

To evaluate the fractures and permeability by using Stoneley wave reflection, it is important to know the effects of pore fluids. To examine the effects of pore fluids, we consider a fluid-filled borehole surrounded by a permeable zone sandwiched between two elastic formations that extend to the surface and the lower infinite half-space, respectively, as shown in Figure 1. Each layer is described by its parameters: compressional velocity (v_p), shear velocity (v_s) and density (ρ). The logging tool is simulated as a rigid cylinder of radius r_t at the borehole center. The logging signals are assumed to be at frequencies below the cut-off frequency of any mode other than the fundamental, so that only the Stoneley wave is excited in the borehole. As the Stoneley wave is a guided wave, most of the energy is trapped inside the borehole. There is almost no geometrical spreading, and at such a low frequency, borehole fluid may be considered as approximately uniform across the fluid annulus between the tool and the borehole wall (Tang and Cheng, 1993). Under these conditions it is sufficient to solve the problem as a case of one-dimensional wave propagation.

The wave equation for the Stoneley wave is given in terms of displacement potentials,

$$\frac{\partial^2 \phi_i}{\partial z^2} + {k_i}^2 \phi_i = 0 \tag{1}$$

where ϕ_i is the Stoneley wave displacement potential and k_i is the axial Stoneley wavenumber in each layer. The fluid pressure P and the axial displacement u of the Stoneley wave are given by

$$P = \rho_f \omega^2 \phi \tag{2}$$

$$u = \frac{\partial \phi}{\partial z} \tag{3}$$

where ρ_f is fluid density and ω is angular frequency.

The solution to Eq. (1) is given by

$$\phi_i = D_i e^{ik_i z} + U_i e^{-ik_i z} \tag{4}$$

where D_i and U_i are unknown coefficients at each layer. The first term of Eq. (4) represents the down-going wave and the second term represents the up-going wave. Let us consider each of the boundaries in turn. At boundary I, a down-going Stoneley wave $D_1 e^{ik_1 z}, (z < z_1)$ is incident at the boundary. In the upper layer, there are both incident and reflected waves, since some part of the energy of the incident wave will be reflected back from the boundary. Therefore, the potential in the upper layer is given by

$$\phi_1 = D_1 e^{ik_1 z} + U_1 e^{-ik_1 z}$$

where D_1 and U_1 are the amplitude coefficients for the incident and the reflected waves, respectively.

In the lower layer, there are only transmitted waves but no up-going waves because the lower layer is an infinite half space and there is no source.

$$\begin{aligned} \phi_2 &= D_2 e^{ik_2 z} + U_2 e^{-ik_2 z} \\ &= D_2 e^{ik_2 z} \end{aligned}$$

where D_2 is the amplitude coefficient of the transmitted wave. The two unknown coefficients U_1 and D_2 are determined from the boundary conditions.

Following the model of Tezuka *et al.* (1994), the coupling inside the borehole is caused by the differences among the k_i propagation constants and the change in the borehole radius as well. Then, we have to consider the boundary condition of mass balance. The mass balance means that the volume of the fluid squeezed from the upper layer should be equal to the volume of the incoming fluid in the lower layer. That is,

$$a_1 u_1(z_1) = a_2 u_2(z_1) \tag{5}$$

where a_1 and a_2 are section areas of each layers; $u_1(z_1)$ and $u_2(z_1)$ are vertical displacements at $z = z_1$ given by Eq. (3). The mass balance condition provides the following simultaneous equations through Eqs. (5), (2), and (3):

$$\begin{aligned} D_1 e^{ik_1 z_1} + U_1 e^{-ik_1 z_1} &= D_2 e^{ik_2 z_1} \\ a_1 k_1 (D_1 e^{ik_1 z_1} - U_1 e^{-ik_1 z_1}) &= a_2 k_2 D_2 e^{ik_2 z_1}. \end{aligned}$$

These equations can be solved for unknown coefficients U_1 and D_2.

$$\begin{aligned} U_1 &= \frac{a_1 k_1 - a_2 k_2}{a_1 k_1 + a_2 k_2} e^{2ik_1 z_1} D_1 \\ D_2 &= \frac{2a_1 k_1}{a_1 k_1 + a_2 k_2} e^{i(k_1 - k_2) z_1} D_1. \end{aligned} \tag{6}$$

At $z = 0$ the reflection (R) and transmission (T) coefficients are given by

$$\begin{aligned} R = U_1/D_1 &= \frac{a_1 k_1 - a_2 k_2}{a_1 k_1 + a_2 k_2} \\ T = D_2/D_1 &= \frac{2a_1 k_1}{a_1 k_1 + a_2 k_2}. \end{aligned} \tag{7}$$

The wavenumber k of the Stoneley wave in the fluid-filled borehole, surrounded by an elastic formation and containing a rigid tool at the borehole center, is determined by the following borehole period equation (Schmitt, 1988; Tang and Cheng, 1991).

$$\begin{aligned} \frac{I_0(fr)}{I_1(fr)} &+ \frac{I_1(fr_t)}{I_1((fr)} \frac{K_0(fr)}{K_1((fr_t)} + \left\{ 1 - \frac{I_1(fr_t)}{I_1((fr)} \frac{K_1(fr)}{K_1((fr_t)} \right\} \\ &\times \frac{\rho}{\rho_f} \frac{f}{l} \left[(\frac{2v_s^2}{c^2} - 1)^2 \frac{K_0(lr)}{K_1((lr_t)} - \frac{2v_s^2 lm}{c^2 k^2} \left\{ \frac{1}{mr} + \frac{2v_s^2}{c^2} \frac{K_0(mr)}{K_1((mr)} \right\} \right] = 0 \end{aligned} \tag{8}$$

where I_n and K_n are the first and second kind modified Bessel functions of order n ($n = 0, 1$), ρ is formation density, ρ_f is fluid density, $c = \omega/k$ is the Stoneley wave phase velocity and r and r_t are the borehole and tool radii, respectively. The radial wavenumbers, l, m and f are given by

$$\begin{aligned} l &= \sqrt{k_2 - \omega_2/v_p^2} \\ m &= \sqrt{k_2 - \omega_2/v_s^2} \\ f &= \sqrt{k_2 - \omega_2/v_f^2}. \end{aligned}$$

Given the elastic properties of the respective layers, the Stoneley wavenumber k can be determined as a function of frequency.

To calculate the synthetic waveforms, we need the Stoneley incident amplitude $A(\omega)$ which is related to the source and the excitation function. At the source position, it is given by

$$A(\omega) = S(\omega) E(\omega) \tag{9}$$

where $S(\omega)$ is the source spectrum and $E(\omega)$ is the Stoneley wave excitation function that is given by Tang and Cheng (1993). The excitation function of the Stoneley wave is a function that depends on the formation and fluid properties, and on the borehole radius and the tool radius. This function is usually calculated by a discrete wavenumber summation technique; however we are interested in only the Stoneley but not other modes, so that the excitation function can be calculated by the Residue Theorem (Kurkjian, 1985). Putting $D_1(\omega) = A(\omega)$, using the solved amplitude coefficients ($U_i(\omega)$, $D_i(\omega)$), the fluid pressure [from Eqs. (2) and (3)] at specific receiver positions is calculated as a function of the frequency. The results are then transformed into the time domain using an inverse Fourier transform.

$$\begin{aligned} D(t,z) &= \frac{1}{2\pi}\int_{-\infty}^{\infty} P(\omega,z)e^{i\omega t}d\omega \\ &= \frac{\rho_f}{2\pi}\int_{-\infty}^{\infty} \omega^2\phi(\omega,z)e^{i\omega t}d\omega \end{aligned}$$

A similar treatment can be made for the boundary II by just swapping the two formations at the boundary. The technique adopted here can be applied to the borehole with various radii in a the multi-layered medium, using the propagator matrix (Tezuka, *et al.*, 1994). For the purpose of this study, however, the formation configuration is fixed to the case of one target zone sandwiched between the upper and lower formations of different properties, as shown in Figure 1.

NUMERICAL MODELING PROCEDURE AND RESULTS

Effects of Pore Fluids

The pore fluid properties involved in the modeling are density, viscosity and acoustic velocity. Five groups of parameters are selected, corresponding to saline water, light crude oil, rich hydrocarbon gas, lean hydrocarbon gas, and drilling fluid (water base mud filtrate) with 5% of gas. These data and the references are listed in Table 1. Figure 2 shows the Stoneley wave attenuation versus frequency for different pore fluids, calculated with the formulas of Tang *et al.* (1991). A permeable sandstone formation is assumed to be the target zone. The parameters for this formation are as follows: P-wave velocity V_p=3.5 km/s, S-wave velocity V_s=2.2 km/s, porosity $Por = 0.25$, pore structure constant $\alpha = 3.0$, absolute permeability $\kappa_0 = 0.5$ Darcy and the formation thickness L=1.52 m. It can be seen that Stoneley attenuation increases rapidly as pore fluid viscosity and velocity decrease. Of particular interest is the case for pore fluid containing 5% (in volume) of natural gas, which is probably the most common case during the logging measurements in a gas field, since the Stoneley wave generally interacts with the invaded zone when it is across a permeable gas-bearing formation. The bulk modulus and the P-wave velocity of the pore fluid are calculated using Kuster-Toksözs theory (Toksöz *et al.*, 1976) for a two-phase media; the viscosity is from Archer and Wall (1986). Toksöz *et al.* (1976) studied the bulk modulus and density of one fluid

spread into the other as immiscible inclusions. They found that when a few percent gas inclusions are introduced into the brine, the bulk modulus of the composite fluid drops rapidly to a value close to that of gas because the high compressibility component of the mixture controls the effective compressibility of the composite fluid. If we consider the pore structure of the permeable formation, it is possible that the P-wave velocity of the permeable zone with 1% gas bubbles in saline water phase is lower than the velocity of a pure gas-saturated formation. The viscosity of brine in a reservoir depends on three main factors: pressure, temperature and the concentration of NaCl. The percentage of gas dissolved in water is a function of pressure. The viscosity of pore fluid is also reduced by a small amount of gas inclusions at the reservoir condition (Burcik, 1979; Serra, 1984). The decrease in velocity and viscosity of pore fluid together causes significant Stoneley wave attenuation in a zone with permeability less than 1 Darcy, which is a common value encountered in reservoirs. A few percent gas inclusions have only a small effect on the S-wave and has almost no effect on other types of logs (Serra, 1984). This character may be employed to distinguish a nonfractured permeable zone from a fractured permeable zone with full wave sonic logs.

Figure 3 shows Stoneley velocities versus frequency for five types of pore fluids. These are typical dispersion curves. It also shows that when a few percent gas inclusions are introduced into the pore fluid, Stoneley velocity decreases nearly 20% at a frequency of 1 kHz, while in a 100% natural gas saturated zone, Stoneley velocity decreases only an additional 5%.

Figures 3–7 show the iso-offset waveforms calculated with the five sets of parameters. Substantial attenuation and clear reflection are observed when a few percent gas inclusions are introduced into the pore fluid. The length of the opening on these iso-offset records is about 3.6 m, roughly equal to the thickness of the zone (1.52 m) plus the source-receiver spacing (2.14 m), which is in good agreement with the theoretical prediction of Tang *et al.* (1991). To quantitatively assess the attenuation, the Stoneley wave transmission and reflection coefficients for a residual gas-bearing zone and the amplitude deficit profiles are calculated and shown in Figures 8 and 9. It can be seen that the Stoneley wave amplitude reduces about 80% in the case of pore fluids containing 5% gas and reduces more than 90% in the case of full gas saturation.

Effects of Lithology and The Boundary of a Permeable Zone

Given pore fluid as brine containing 5% gas in volume concentration, we now change the lithology to model the effects of rock matrix and formation boundary on Stoneley wave attenuation and reflection. Two sets of parameters for the permeable zone are selected for these numerical experiments. One data set is for "hard formation," which has almost identical matrix properties to the surrounding formation. This extreme arrangement is made to effectively eliminate the lithology boundaries of the permeable zone under study, and therefore somehow isolates the pore fluid related effects. The second set is chosen for "soft formation", because the S-wave velocity of this formation is well below the P-wave velocity of bore fluid. The lithology contrasts at the boundaries are made to

simulate the other extreme. These parameters are listed in Table 2. Figure 10 shows the total transmission and reflection coefficients calculated for the two cases. Comparing the two sets of numerical results, only about a 5% differences can be observed between coefficients. Both the total transmission and reflection coefficients are higher for the "soft formation" than for the "hard formation." The characteristics of the two sets of curves are very similar. The correspondent iso-offset waveforms are shown in Figures 11 and 12; it is hard to tell the difference between the two waveforms. The effects of permeability and pore fluids on Stoneley wave attenuation are so dominant that the large lithology differences between the two zones (mainly velocity differences between the two formation matrices) have little effect on Stoneley wave propagation.

Effects of Porosity and Permeability

Porosity and pore structure (tortuosity) are correlated to formation permeability in a complex fashion. Tortuosity usually equals 3 for porous media and 1 for fractures. A 3% connected fracture porosity may result in quite high permeability, while a porosity of 20% for a nonfractured sandstone formation usually gives a permeability less than 1 Darcy. Tang *et al.* (1991) examined the effects of tortuosity on Stoneley wave attenuation. Their results demonstrated that at low frequencies (say, less than 2 kHz), changes in tortuosity value have little effect on Stoneley attenuation. Given tortuosity equal to 3 and pore fluids and other formation properties the same as those used in the previous section, we now change the porosity and permeability of the target zone to see what the critical values are where Stoneley attenuation and reflection become evident. In other words, what is the resolution for determining permeability under these conditions? Figure 13 gives the total transmission and reflection coefficients calculated for five sets of evaluated porosity and permeability pairs, keeping the other parameters constant. These values are typical for moderate to low permeability sandstone formations. The central frequency chosen for Stoneley excitation is 1 kHz. At this frequency, the transmission and reflection coefficients are equal when the porosity is 0.2 and permeability is 0.4 Darcy. As porosity and permeability increase further, the transmission coefficients become smaller than the reflection coefficients and the difference between them increase synchronously. Figure 14 shows the amplitude deficit profiles calculated for these cases. It shows that the largest relative increase in deficit occurred when porosity was increased from 0.1 to 0.2 and permeability from 0.2 Darcy to 0.4 Darcy. Figures 15 and 16 show the results from similar calculations for fully gas-saturated formations of permeabilities from 100 milliDarcy to 1 milliDarcy. It is seen from these figures that substantial Stoneley wave attenuation and reflection are observed in a zone with a permeability of only 5 milliDarcies. Stoneley wave reflection is still noticeable when the permeability of the zone is only 1 milliDarcy. The deficit value of Stoneley amplitude is also controlled by the thickness of the permeable zone. This is explained below.

Effects of the Thickness of a Permeable Zone

Tang *et al.* (1991) have shown that Stoneley transmission loss at high frequencies is an increasing function of the product of zone thickness with porosity. We examine this effect at lower frequencies under the conditions defined previously. We want to find out the resolution in terms of the thickness that can be achieved by Stoneley amplitude data under the permeable zone and pore fluid conditions described here. Figure 17 gives Stoneley amplitude deficit profiles for four values of zone thickness, with all other parameters remaining the same. It can be seen that Stoneley wave amplitude is attenuated by over 50% when the zone thickness is larger than 0.5 meters. The reflection coefficients calculated for these cases are shown in Figure 18. The average reflection coefficient at frequencies around 1 kHz is about 0.1 for thickness $L = 0.5$ m. With this reflection coefficient value, the reflection energy of the zone should be evident in the iso-offset waveform record. These numerical experiments demonstrate that, under the conditions considered here (essentially, typical sandstone parameters), Stoneley wave attenuation and reflection can be observed for a permeable zone that is thicker than 0.5 meters.

SUMMARY AND CONCLUSIONS

We have examined the sensitivities of the modeling method developed by Tang *et al.* (1991) for determining the permeability of a permeable zone with Stoneley wave attenuation and reflection data. There is no doubt about the usefulness of Stoneley wave attenuation and reflection data in detecting fractures and fractured permeable zones. We examine the relative effects due to these formation properties, other than fracture permeability, to make better use of numerical technology in processing field measurements, especially for data from natural gas fields. This study may be used as part of extensive testing for applying new numerical technology to logging practices. The effects of pore fluid, porosity, lithologies of surrounding formation, and the thickness of a target zone on Stoneley wave amplitude are systematically modeled in this study for permeable sandstone zones. The sensitivity of Stoneley wave propagation to these conditions is assessed quantitatively. It is found that the presence of light hydrocarbon in the formation, especially natural gas residuals in the immediate vicinity of the borehole wall, even with only 5% contained in pore fluid, may also cause substantial Stoneley attenuation and reflection. For the full gas-saturated zone, Stoneley wave reflection may be observed even when permeability is as low as a few milliDarcies. Compared to the effects of pore fluid, the effects due to lithology contrasts at the boundaries and the change of nonfracture porosity are insignificant in the cases studied here. For a residual gas-bearing zone of moderate permeability, such as those encountered in typical sandstone reservoirs, Stoneley wave attenuation and reflection may be observed if the zone is thicker than 0.5 meter.

ACKNOWLEDGMENTS

This research was supported by the Borehole Acoustics and Logging Consortium at M.I.T.'s Earth Resources Laboratory, the ERL/nCUBE Geophysical Center for Parallel Processing, and DOE Contract #DE-FG02-86ER13636.

REFERENCES

Archer, J.S. and Wall, C.G., 1986, *Petroleum Engineering: Principles and Practice,* Graham and Trotman, Ltd., London.

Biot, M.A., 1962, Mechanics of deformation and acoustic wave propagation in porous media, *J. Appl. Phys., 33*, 1482–1498.

Burcik, E.J., 1979, *Properties of Petroleum Reservoir Fluids,* International Human Resources Development Corp., Boston.

Burns, D.R., Acoustic waveform logs and the in-situ measurement of permeability—A review, Geophysical Applications for Geotechnical Investigations, ASTM STP 1101, F.L. Paillet and W.R. Saunders (Eds.), *American Society for Testing and Materials,* Philadelphia, 1990, 65–78.

Cheng, N.Y., and C.H., Cheng, 1991, Borehole Stoneley wave inversion for formation parameters, *Expanded Abstracts,* SEG Annual Conference, Houston, TX.

Hardin, E.L., Cheng, C.H., Paillet, F.L. and Mendelson, J.D., 1987, Fracture characterization by means of attenuation and generation of tube waves in fractured crystalline rock at Mirror Lake, New Hampshire, *J. Geophys. Res., 92*, 7989–8006.

Hornby, B.E., Johnson, D.L., Winkler, K.H. and Plumb, R.A., 1989, Fracture evaluation using reflected Stoneley-wave arrivals, *Geophysics, 54,* 1274–1288.

Johnson, D.L., Koplik, J. and Dashen, R., 1987, Theory of dynamic permeability and tortuosity in fluid-saturated porous media, *J. Fluid Mech., 176*, 379–400.

Norris, A.N., 1989, Stoneley-Wave attenuation and dispersion in permeable formations, *Geophysics, 54*, 330–341.

Paillet, F.L., and White, J.E., 1982, Acoustic models of propagation in the borehole and their relationship to rock properties, *Geophysics, 47*, 1215–1228.

Paillet, F.L., 1980, Acoustic propagation in the vicinity of fractures which intersect a fluid-filled borehole, Trans. SPWLA 21st Ann. Symp., Paper DD.

Reiter, E.C. and Burns, D.R., 1991, Incoherent/coherent wavefield separation: Application to crosshole seismic data, *Expanded Abstracts,* SEG Annual Conference, Houston, TX.

Rosenbaum, J.H., 1974, Synthetic microseismograms: Logging in porous formations, *Geophysics, 39*, 14–32.

Schmitt, D.P., M. Bouchon, and G. Bonnet, 1988, Full-waveform synthetic acoustic logs in radially semiinfinite saturated porous media, *Geophysics, 53*, 807–823.

Serra, O., 1984, Fundamentals of well-log interpretation: 1. The acquisition of logging data, *Developments in Petroleum Science, 15A*.

Tang, X.M., C.H. Cheng, and M.N. Toksöz, 1990, Stoneley wave propagation in a fluid-filled borehole with a vertical fracture, *Geophysics, 56*, 447–460.

Tang, X.M., C.H. Cheng, and M.N. Toksöz, 1991, Dynamic permeability and borehole Stoneley waves: A simplified Biot-Rosenbaum model, *J. Acoust. Soc. Am., 90*, 1632–1646.

Tang, X.M., E.C. Reiter, and D.R. Burns, 1992, Estimating formation shear velocity from dispersive logging waveforms using a model-guided processing technique, *Expanded Abstracts,* SEG Annual Conference, New Orleans.

Tang, X.M. and C.H. Cheng, 1993, Effects of a logging tool on the Stoneley waves in elastic and porous boreholes, *The Log Analyst, 34*, 46–56.

Tang, X.M., and C.H. Cheng, 1994, Fast inversion of formation permeability from Stoneley wave logs using a simplified Biot-Rosenbaum model, M.I.T. Borehole Acoustics and Logging Consortium Annual Report.

Tang, X.M., 1993, A dispersive processing technique for estimating shear wave velocity from dipole and Stoneley wave logs, *Geophysics, 60*, 19–28.

Tao, G., King, M.S. and Nabi-Bidhendi, M., 1995, Ultrasonic wave propagation in dry and brine-saturated sandstones as a function of effective stress: Laboratory measurements and modeling, *Geophys. Prosp., 43*, 299–327.

Tezuka, K., Cheng, C.H. and Tang, X.M., 1994, Modeling of low frequency Stoneley wave propagation in an irregular borehole, M.I.T. Borehole Acoustics and Logging Consortium Annual Report.

Toksöz, M.N., Cheng, C.H. and Timur, A., 1976, Velocities of seismic waves in porous rocks, *Geophysics, 41*, 621–640.

Williams, D.M., 1990, The acoustic log hydrocarbon indicator, *Trans., Soc. Prof. Well Log. Analysts, 24th Ann. Log. Symp., Paper W.*

Williams, D.M., J. Zemanek, F.A., Angona, C.L. Denis, and R.L. Caldwell, 1984, The long space acoustic logging tool, *Trans. Prof. Well Log Analysts, 25th Ann. Log. Symp. Paper T.*

Winkler, K.W., H.L. Liu, and D.L. Johnson, 1989, Permeability and borehole Stoneley waves: Comparison between experiment and theory, *Geophysics, 54*, 66–75.

Zhao, X.M., Toksöz, M.N. and Cheng, C.H., 1994, Stoneley wave propagation across borehole permeability heterogeneities, M.I.T. Borehole Acoustics and Logging Consortium Annual Report.

Table 1. Pore Fluids and their properties used in this study.

Pore fluids	Density g/cc	Velosity km/s	Viscosity cp
Saline water	1.05	1.55	1.1
Light crude oil	0.65	1.34	0.4
Brine with 5% gas	0.97	0.685	0.2
Rich hydrocarbon gas	0.16	0.455	0.025
lLean hydrocarbon gas	0.07	0.405	0.02

References:

1. Archer and Wall (1984).

2. Serra (1984).

3. Toksöz et al. (1976).

Table 2 Velocities used for 'Hard' and 'Soft' formations

formations	Vp (km/s)	Vs (km/s)
Hard	4.5	2.5
Soft	2.5	1.5
Surrounding	4.5	2.5

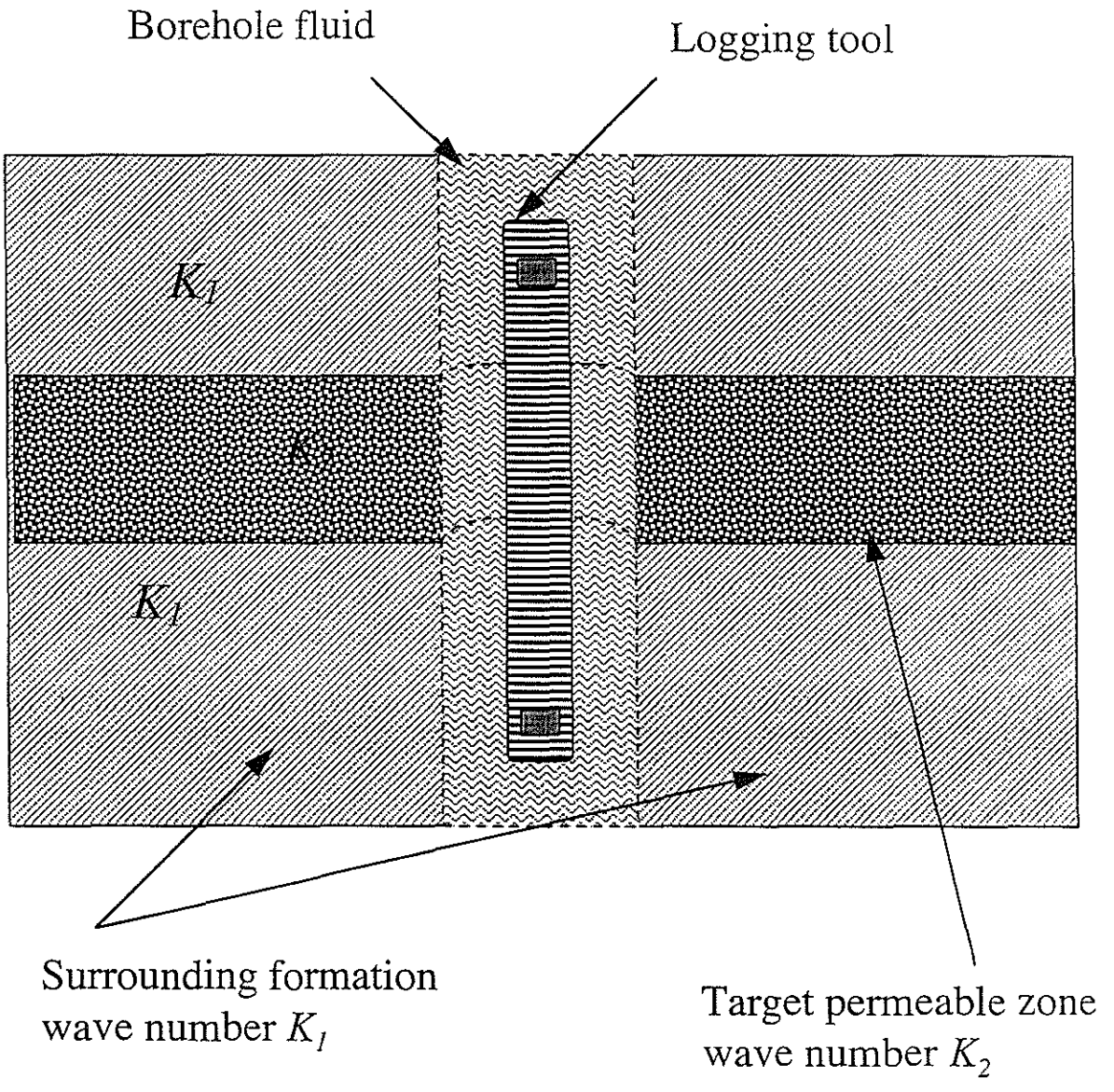

Figure 1: Diagram showing acoustic logging across a permeable zone sandwiched in elastic formations. The interaction of the Stoneley wave and the zone is modeled as due to the different wavenumbers K_1 and K_2 of the zone and the formations.

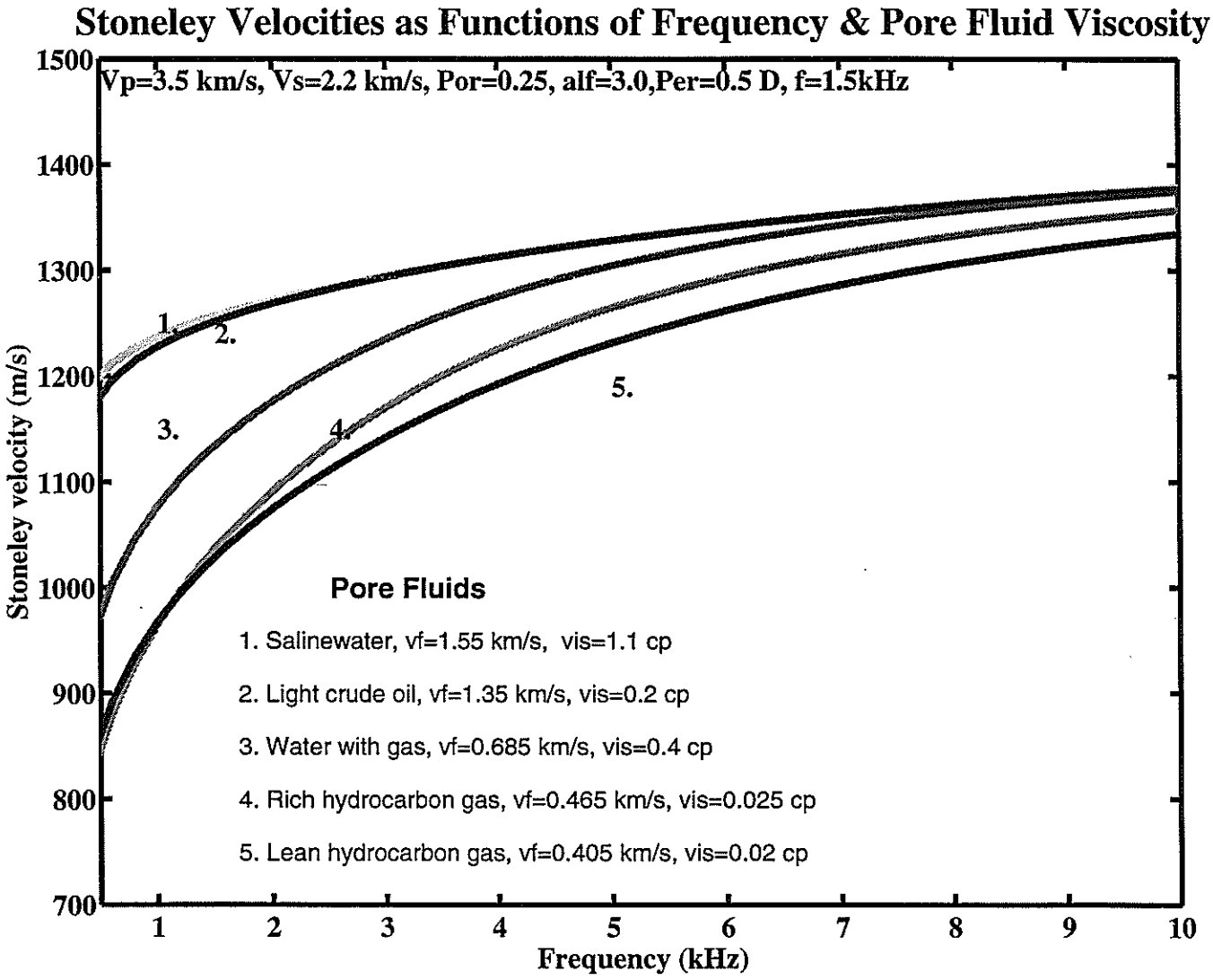

Figure 2a: Stoneley wave velocities as a function of frequency and pore fluids.

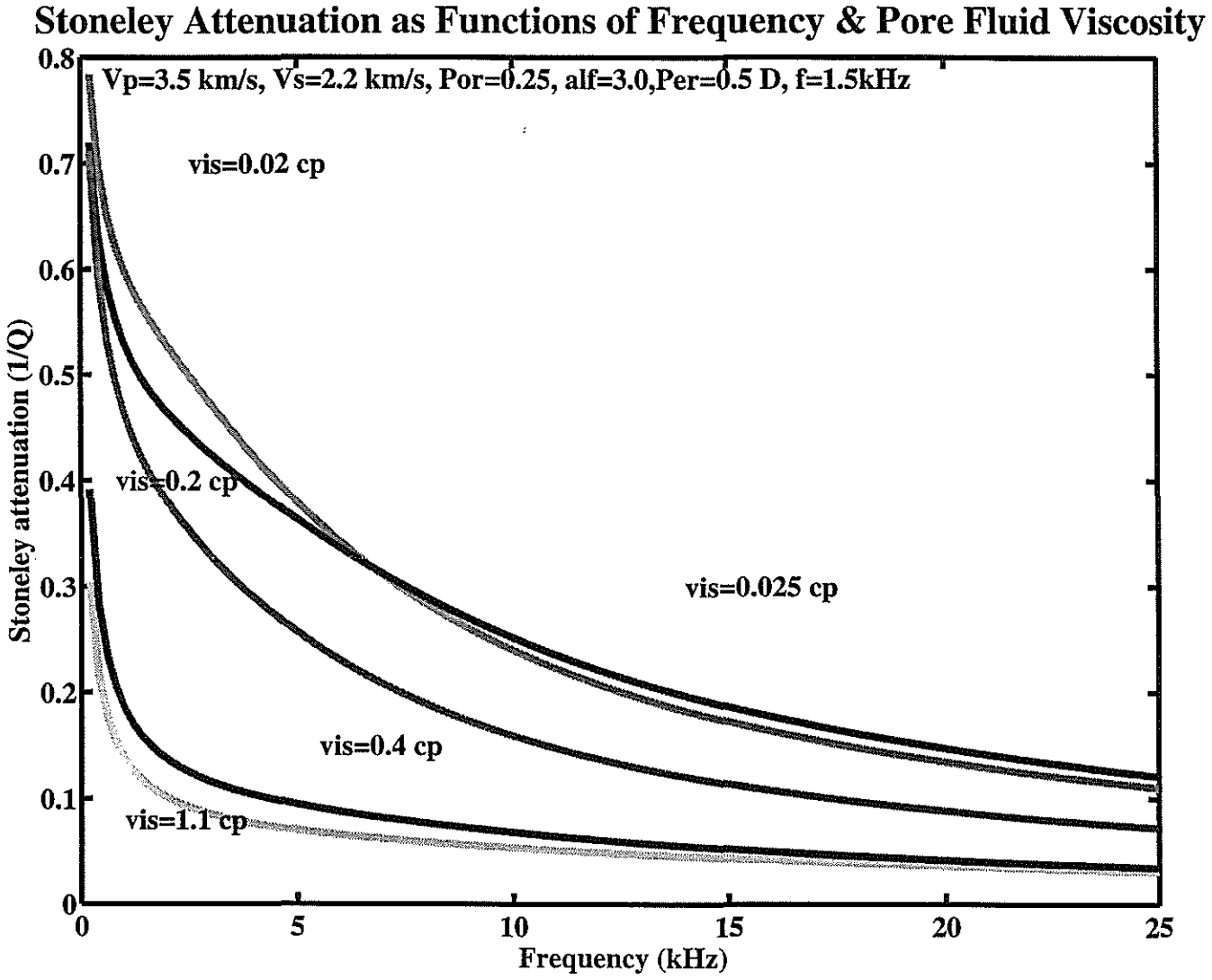

Figure 2b: Stoneley wave attenuation as a function of frequency and pore fluids.

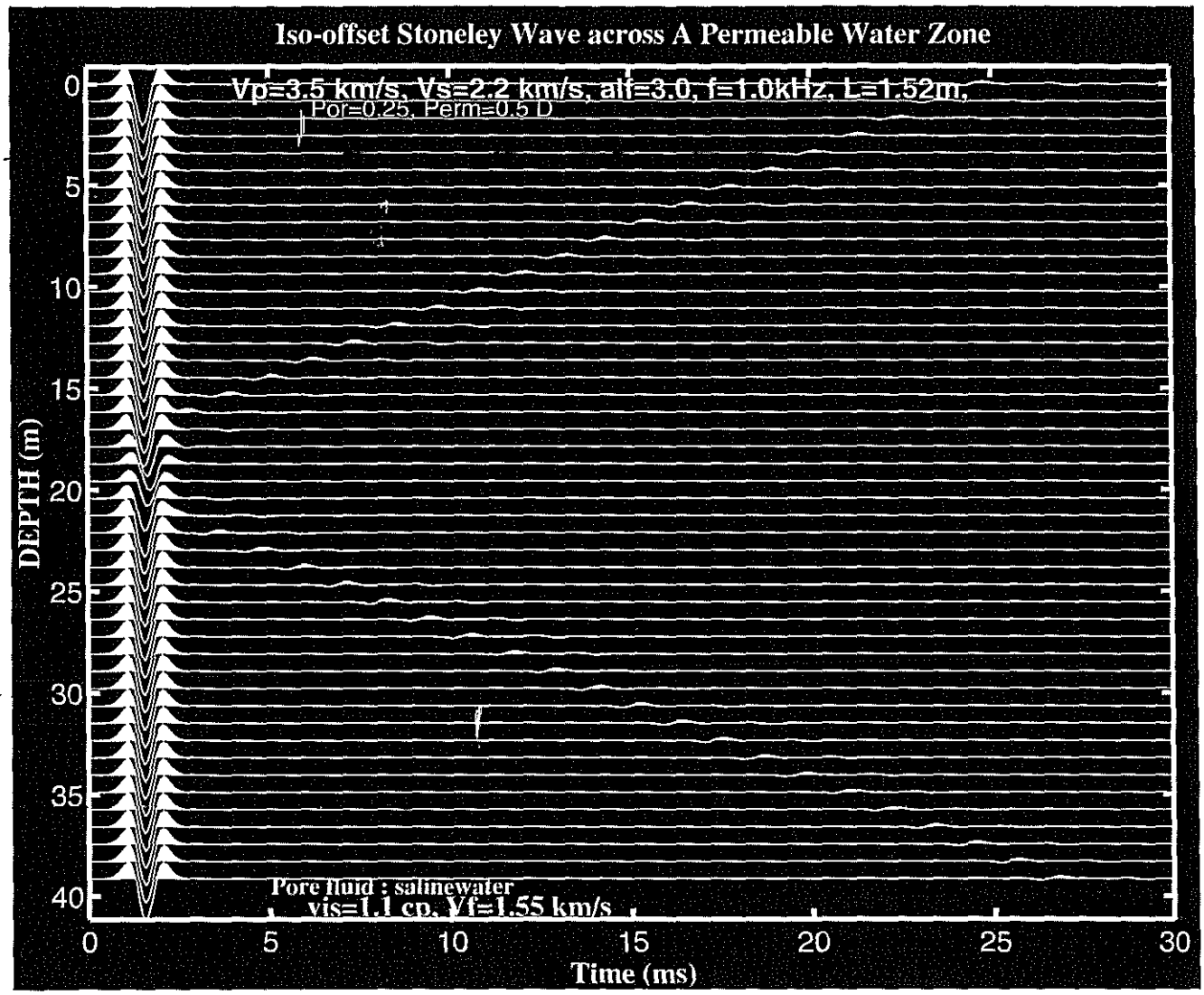

Figure 3: Iso-offset records of a Stoneley wave across a permeable water zone.

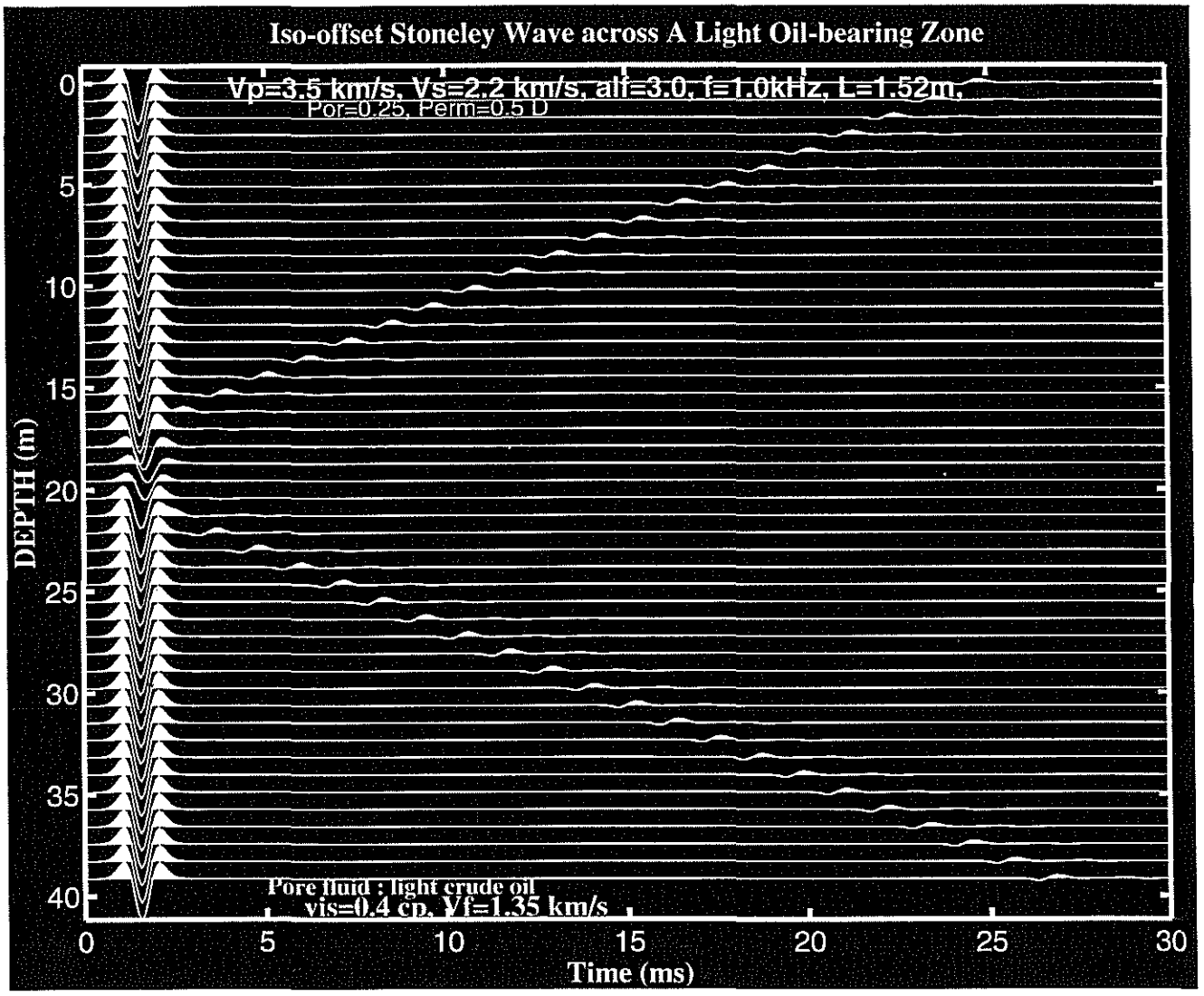

Figure 4: Iso-offset records of a Stoneley wave across a light oil-bearing zone.

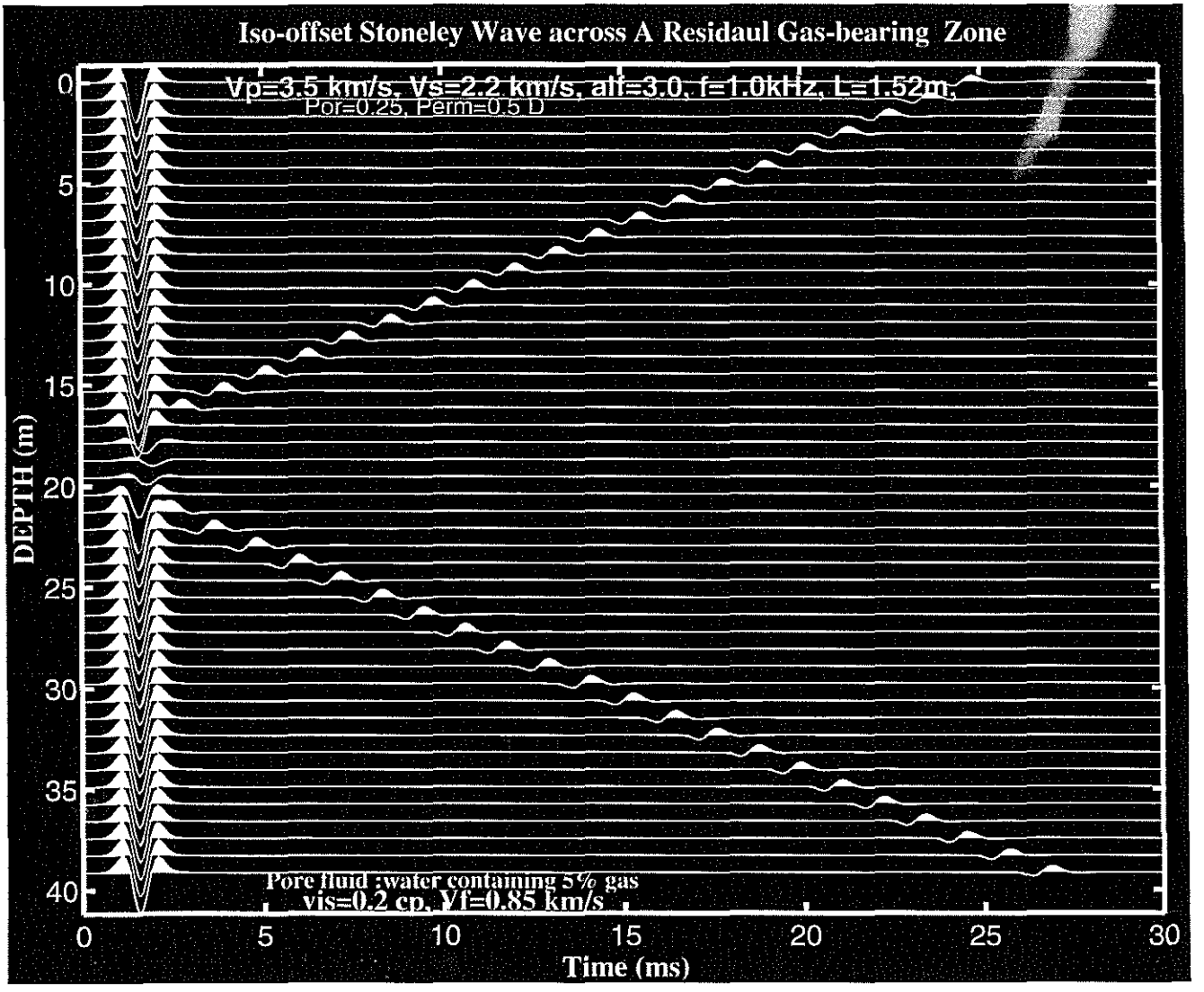

Figure 5: Iso-offset records of a Stoneley wave across a residual gas-bearing zone.

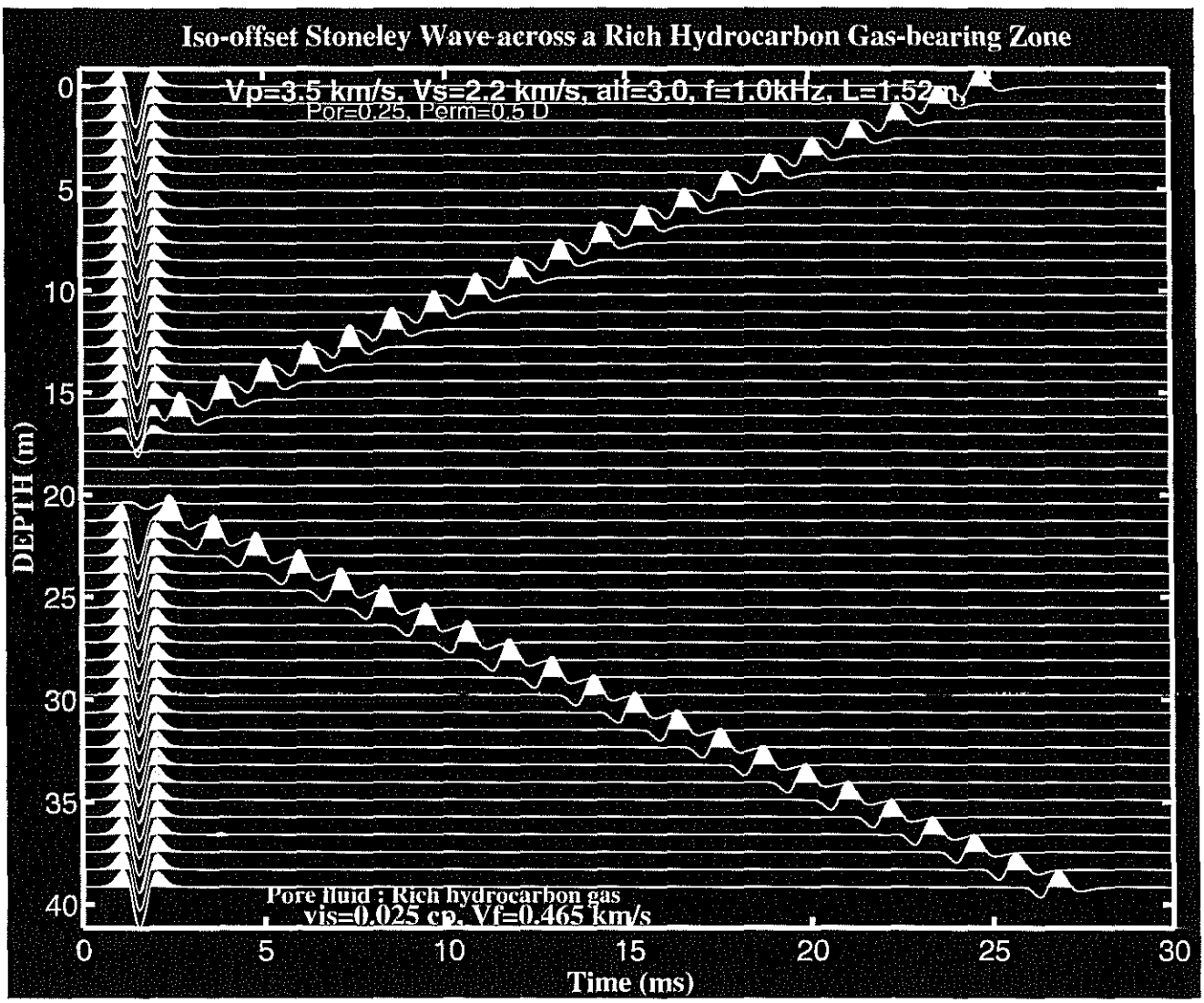

Figure 6: Iso-offset records of a Stoneley wave across a rich hydrocarbon gas-bearing zone.

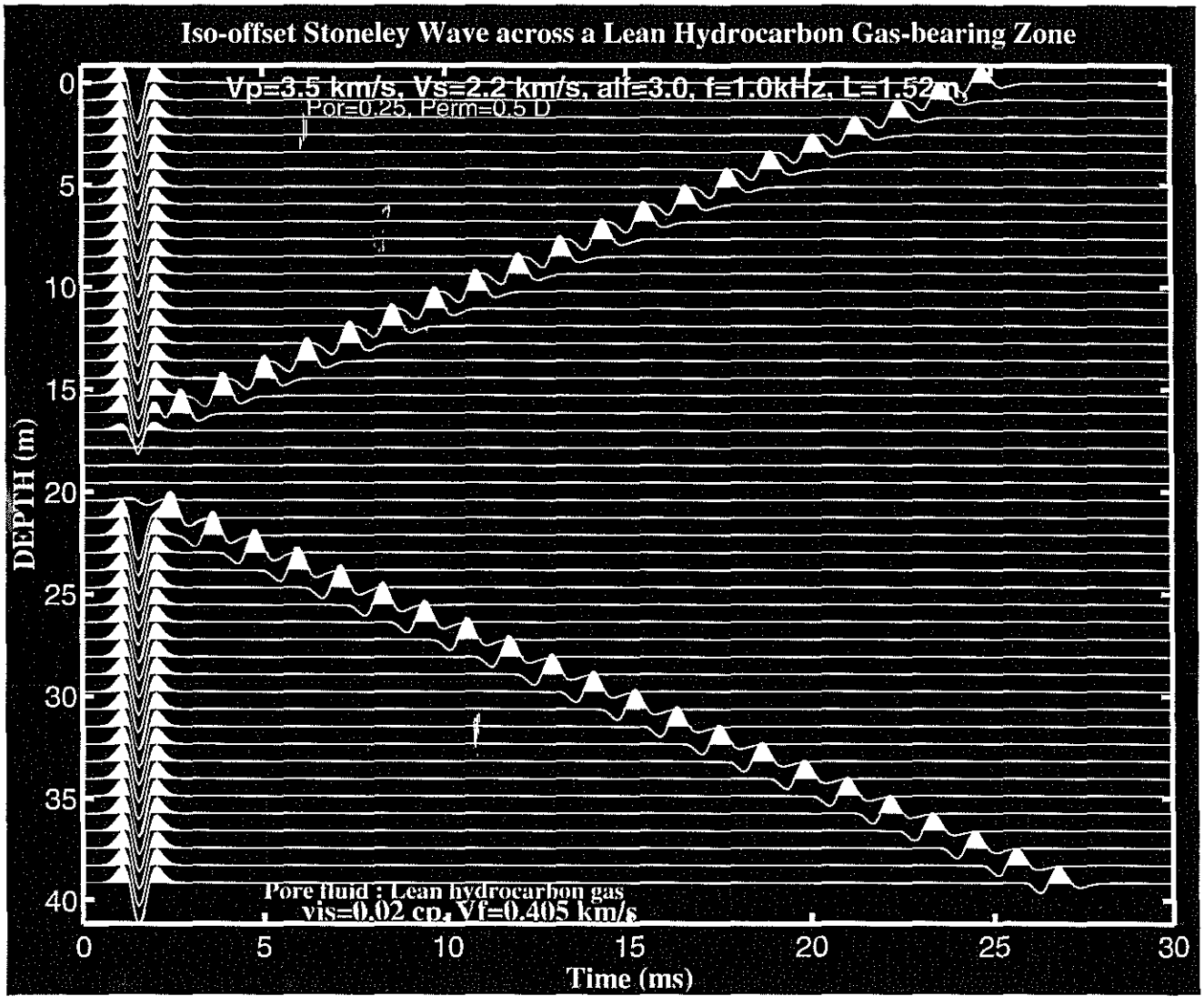

Figure 7: Iso-offset records of a Stoneley wave across a lean hydrocarbon gas-bearing zone.

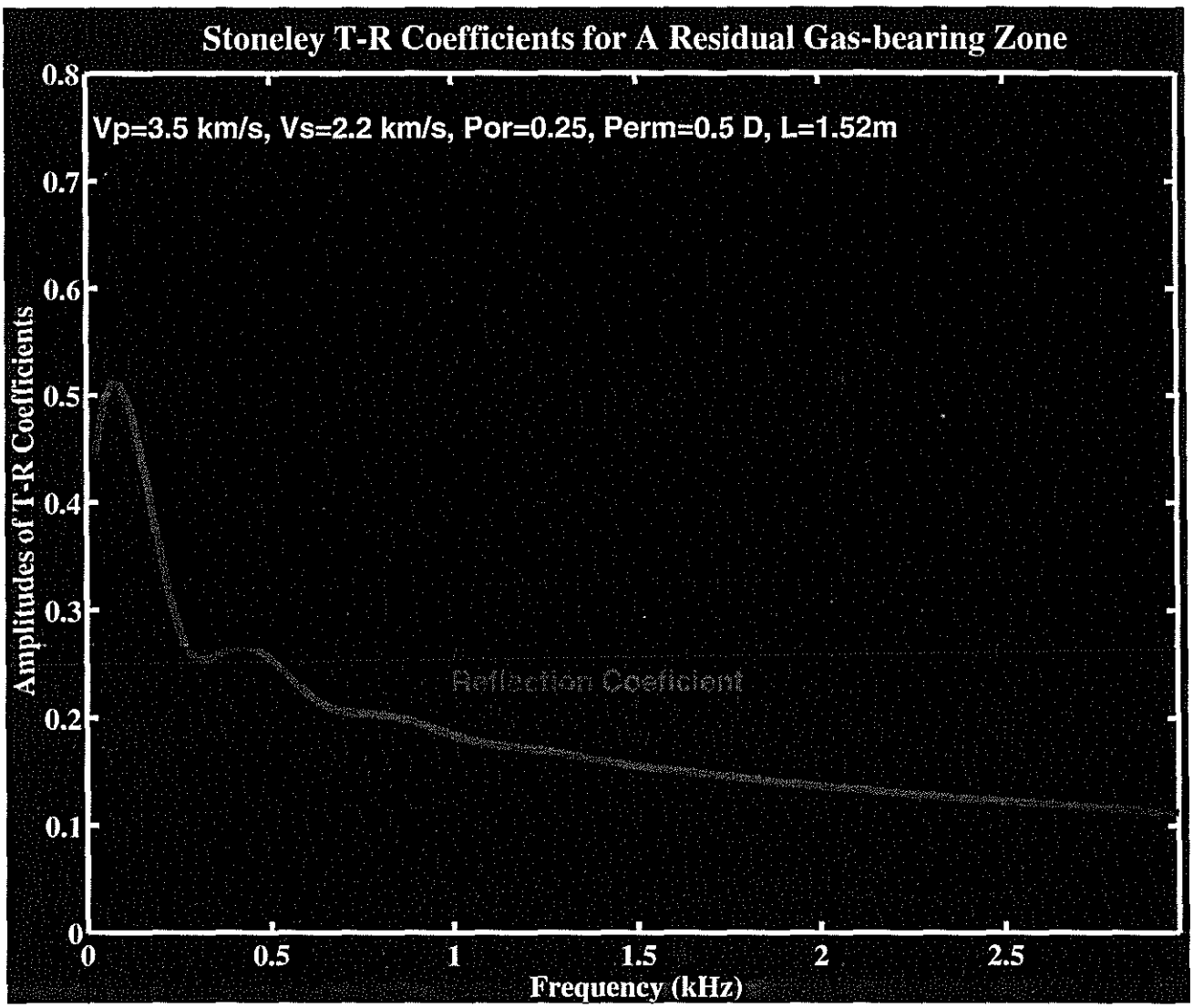

Figure 8: Stoneley wave transmission and reflection coefficients for a residual gas-bearing zone.

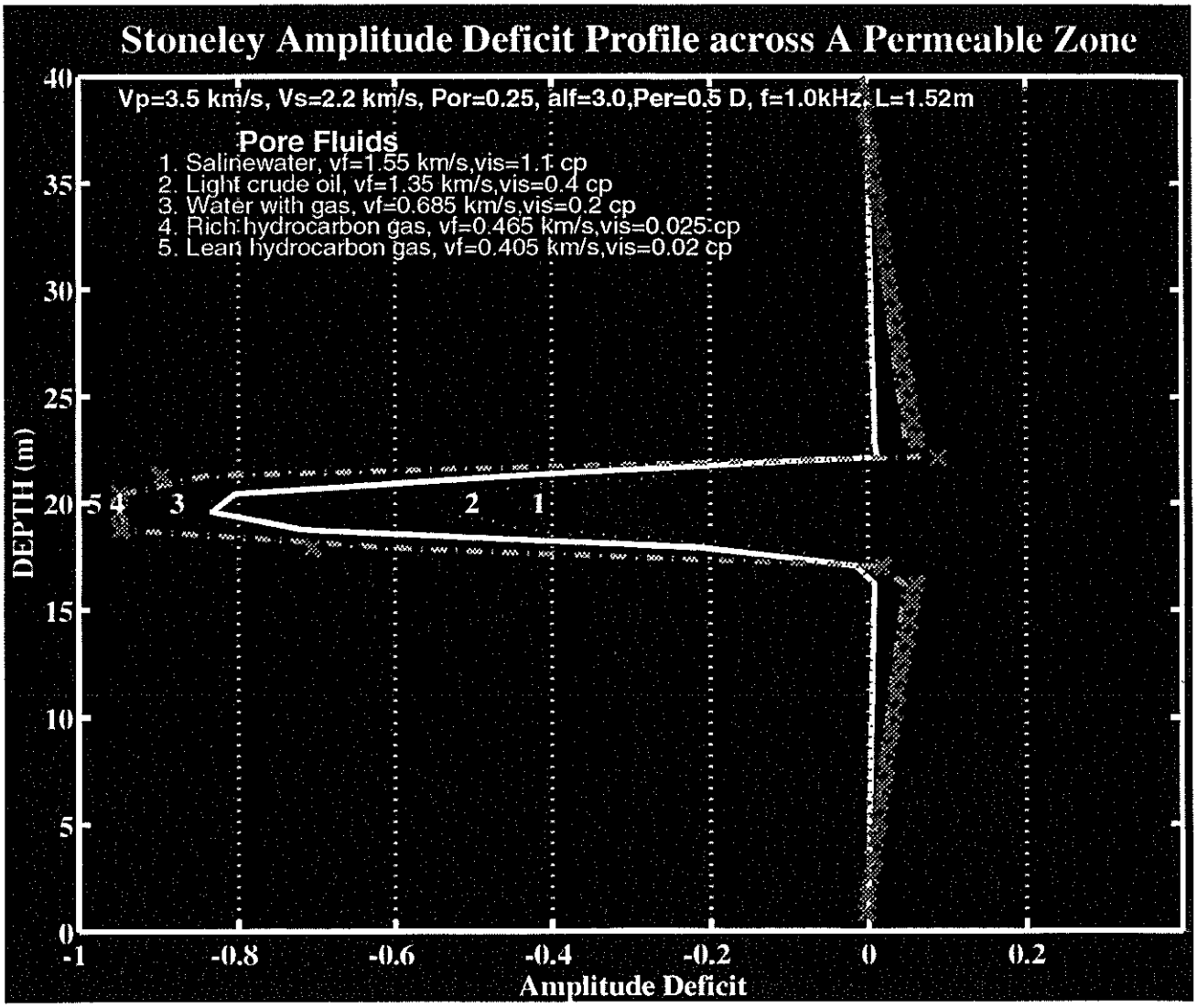

Figure 9: Stoneley wave amplitude deficit profile across a permeable zone containing different pore fluids.

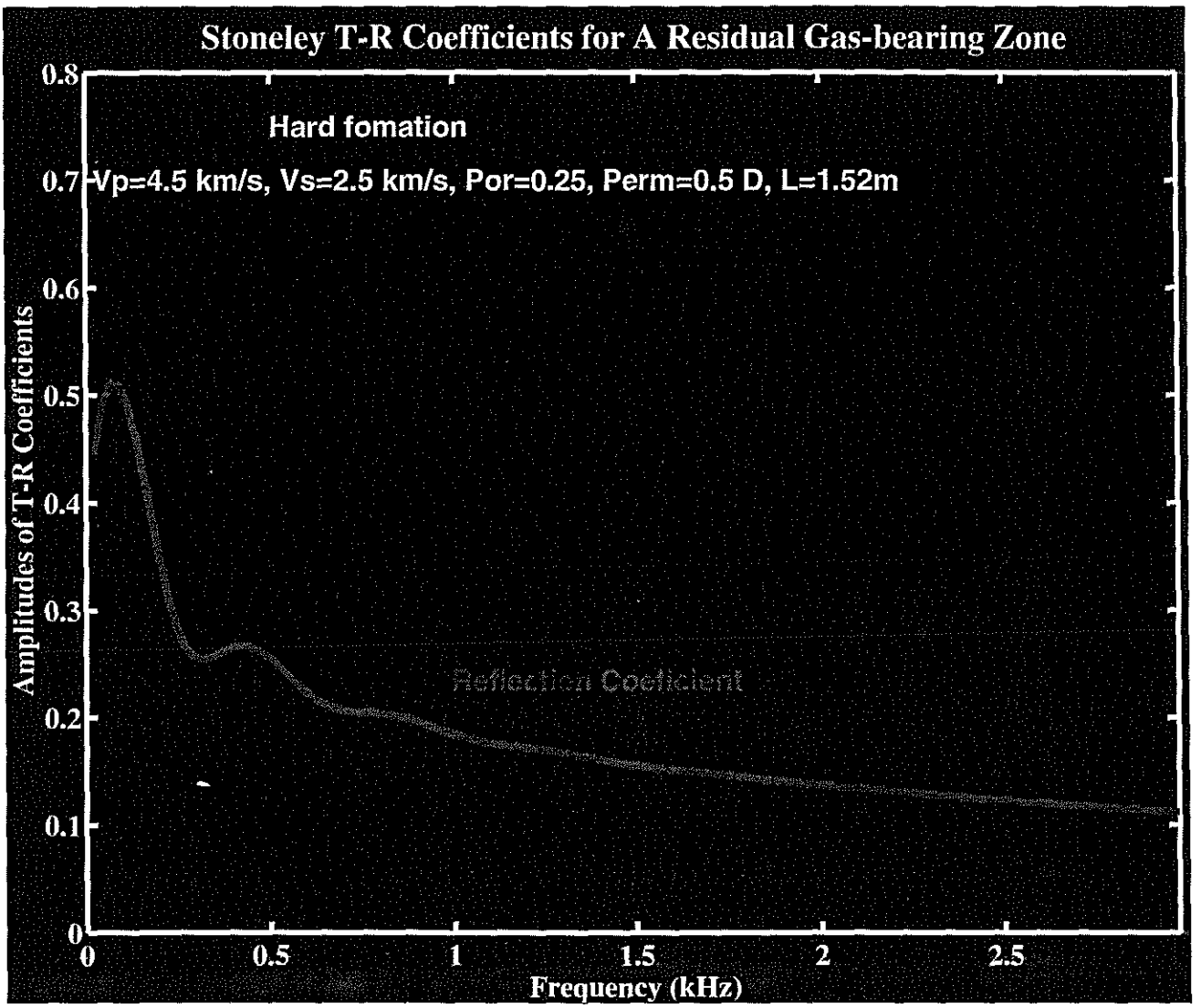

Figure 10: Stoneley wave transmission and reflection coefficients for a residual gas-bearing zone. a. Hard formation.

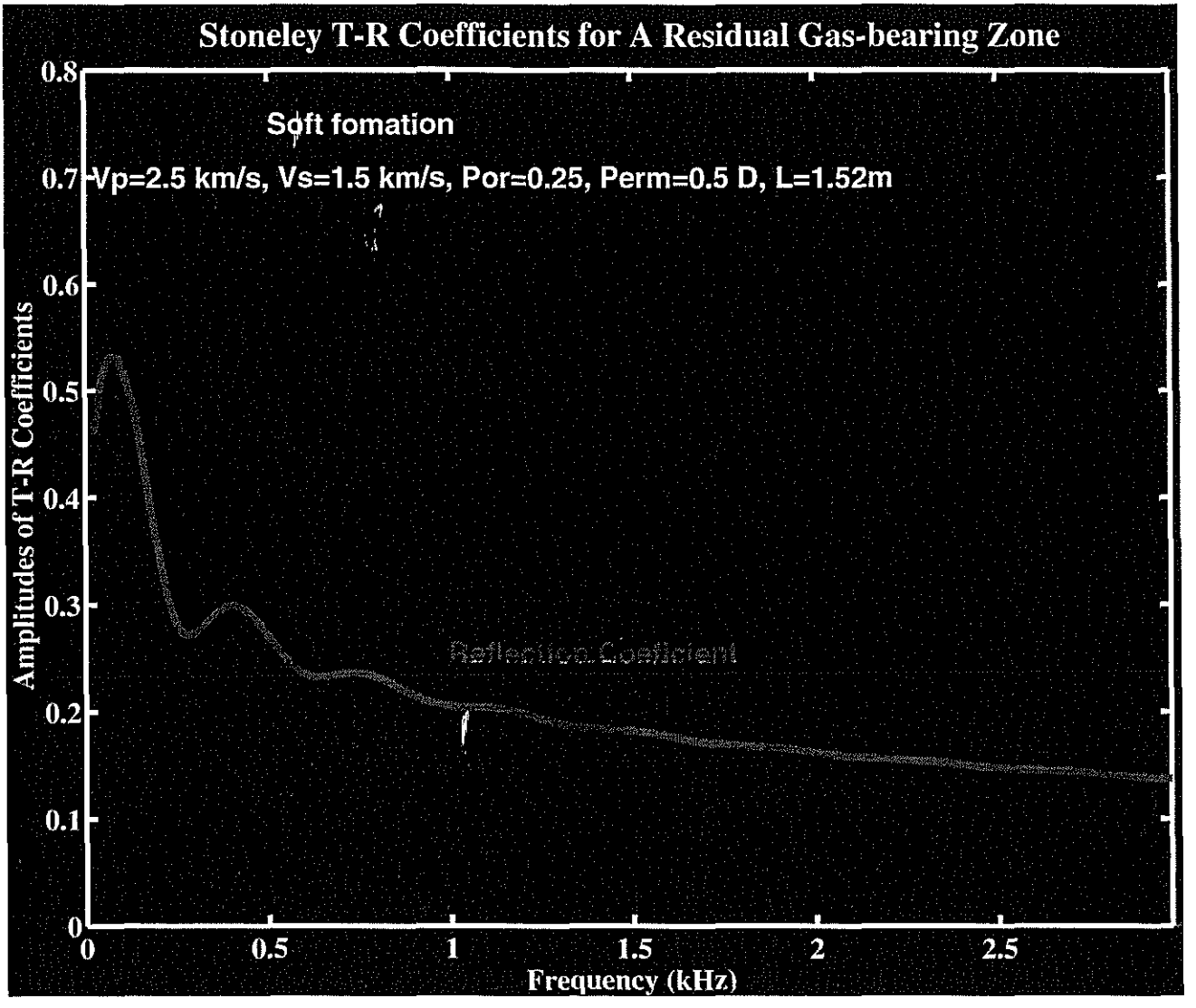

Figure 10b: Stoneley wave transmission and reflection coefficients for a residual gas-bearing zone. b. Soft formation.

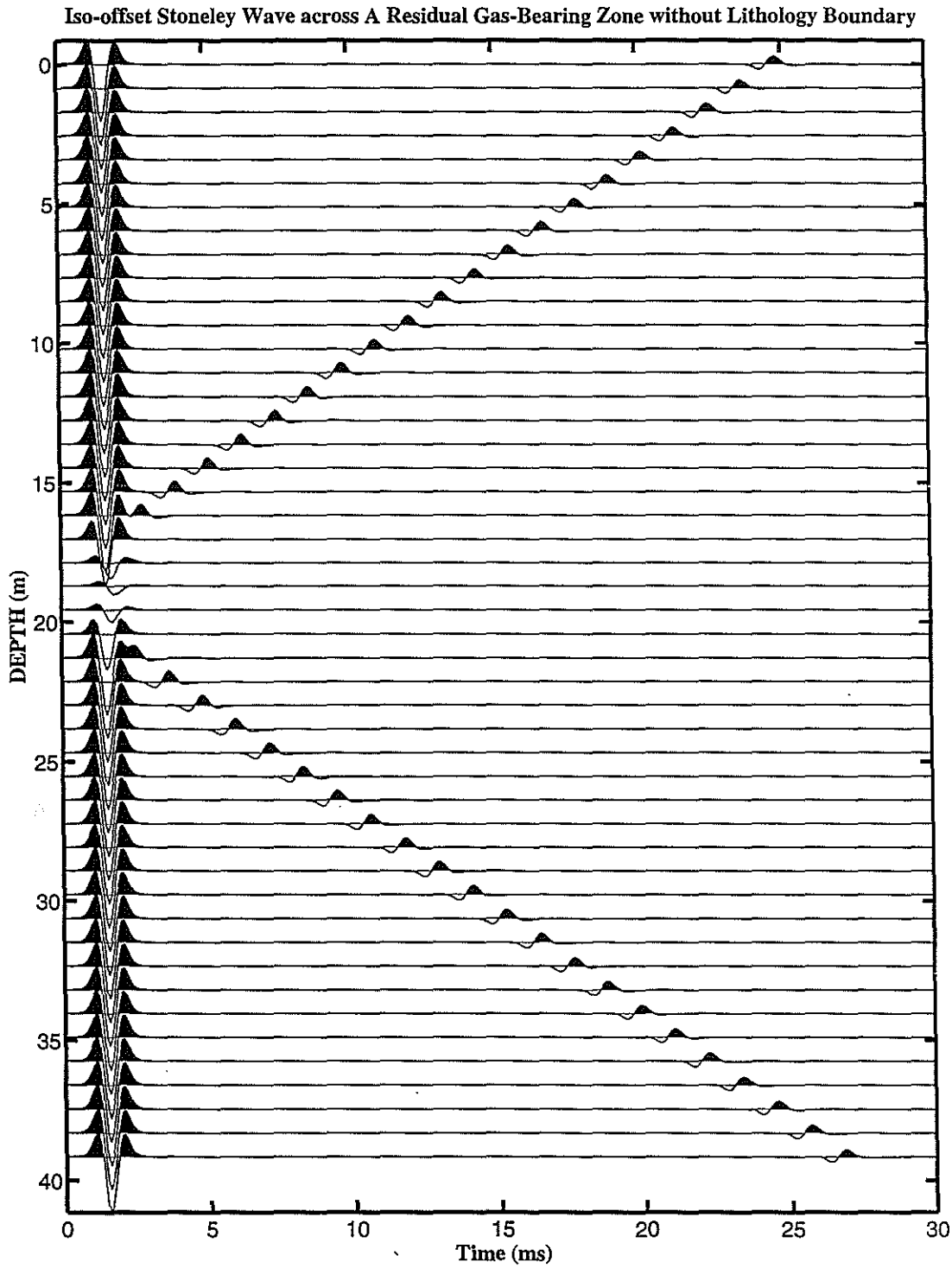

Figure 11: Iso-offset records of a Stoneley wave across a residual gas-bearing zone with a "hard" formation matrix.

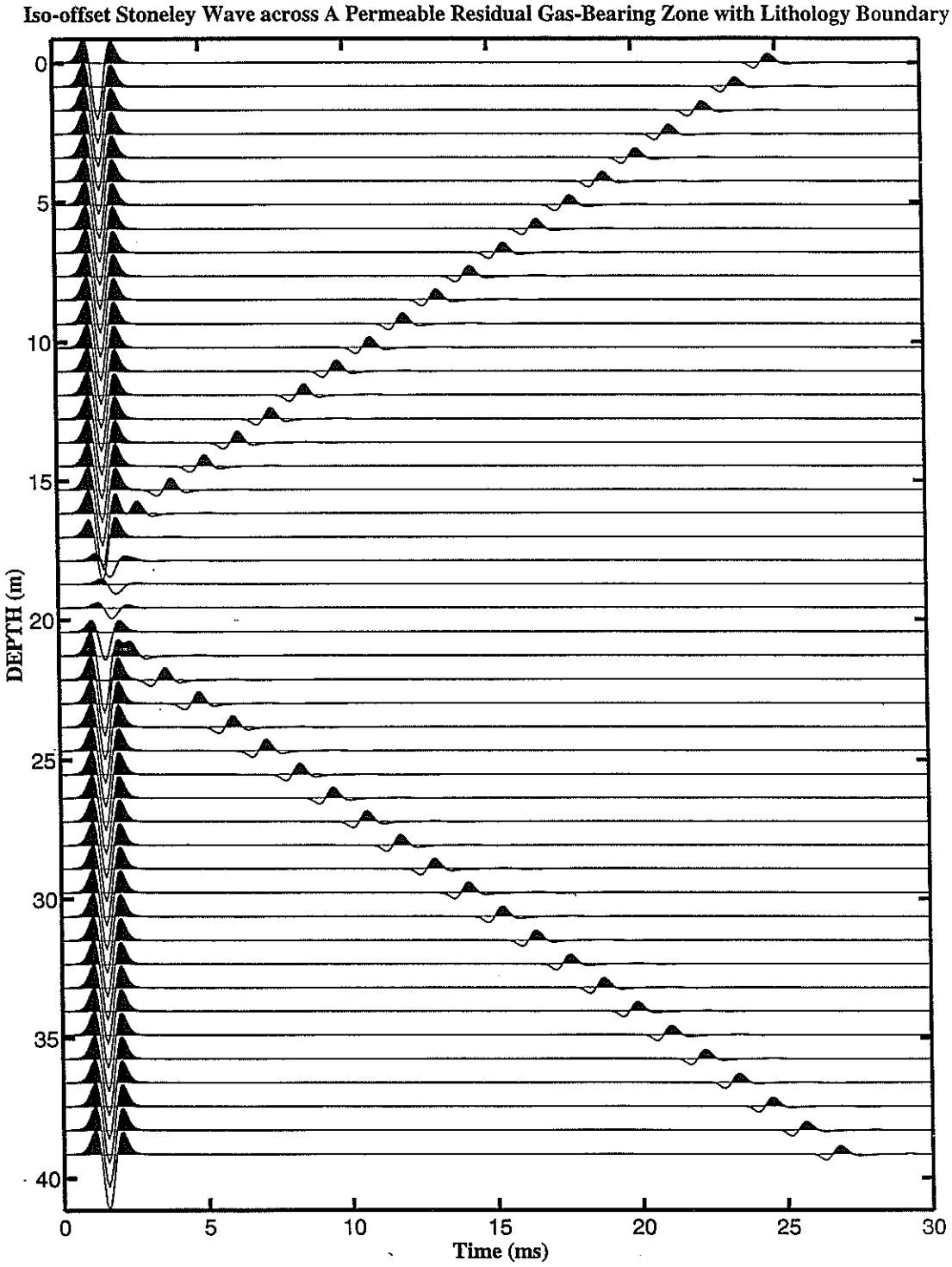

Figure 12: Iso-offset records of a Stoneley wave across a residual gas-bearing zone with a "soft" formation matrix.

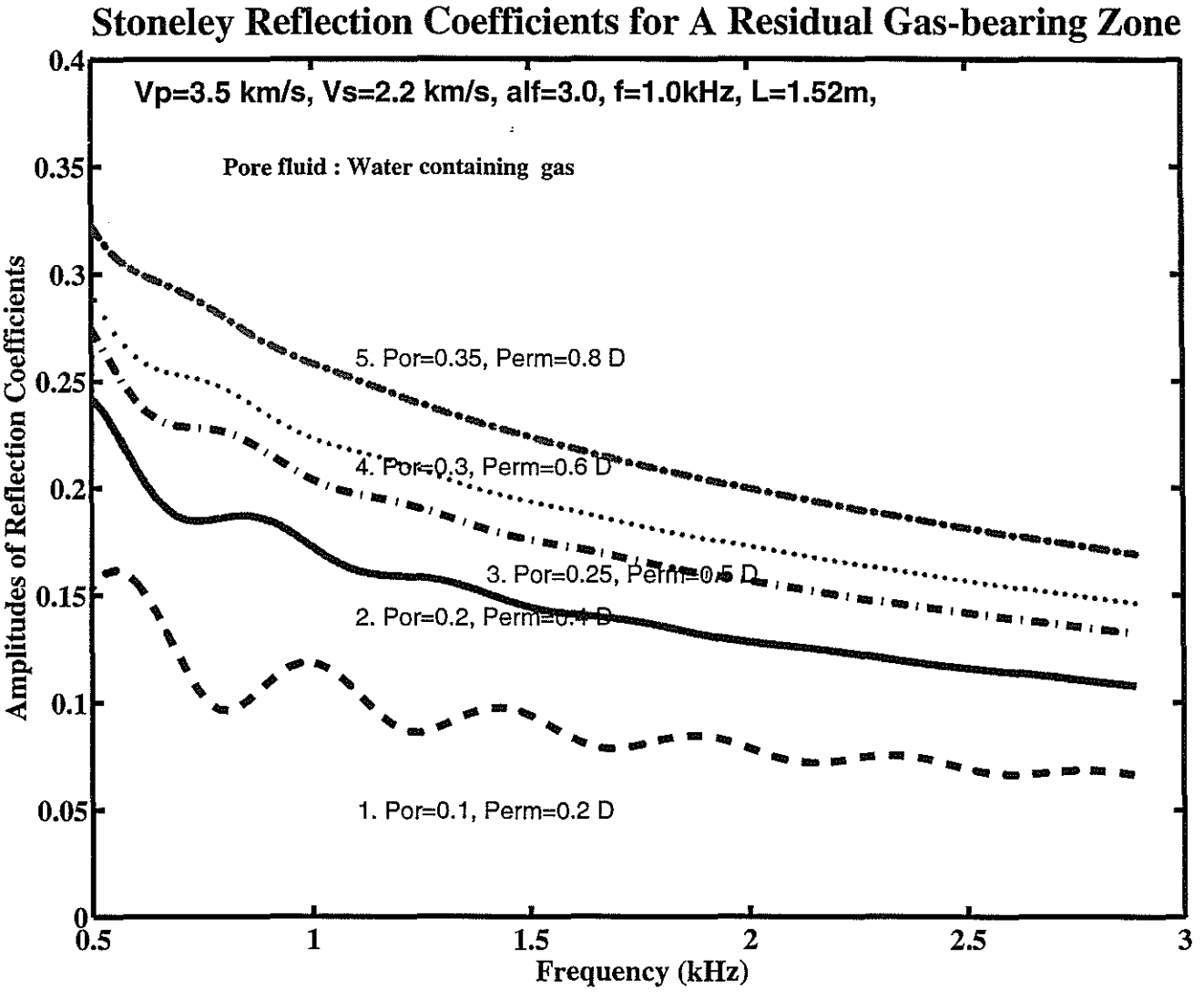

Figure 13a: Stoneley wave transmission and reflection coefficients for a residual gas-bearing zone. a. Reflection coefficients.

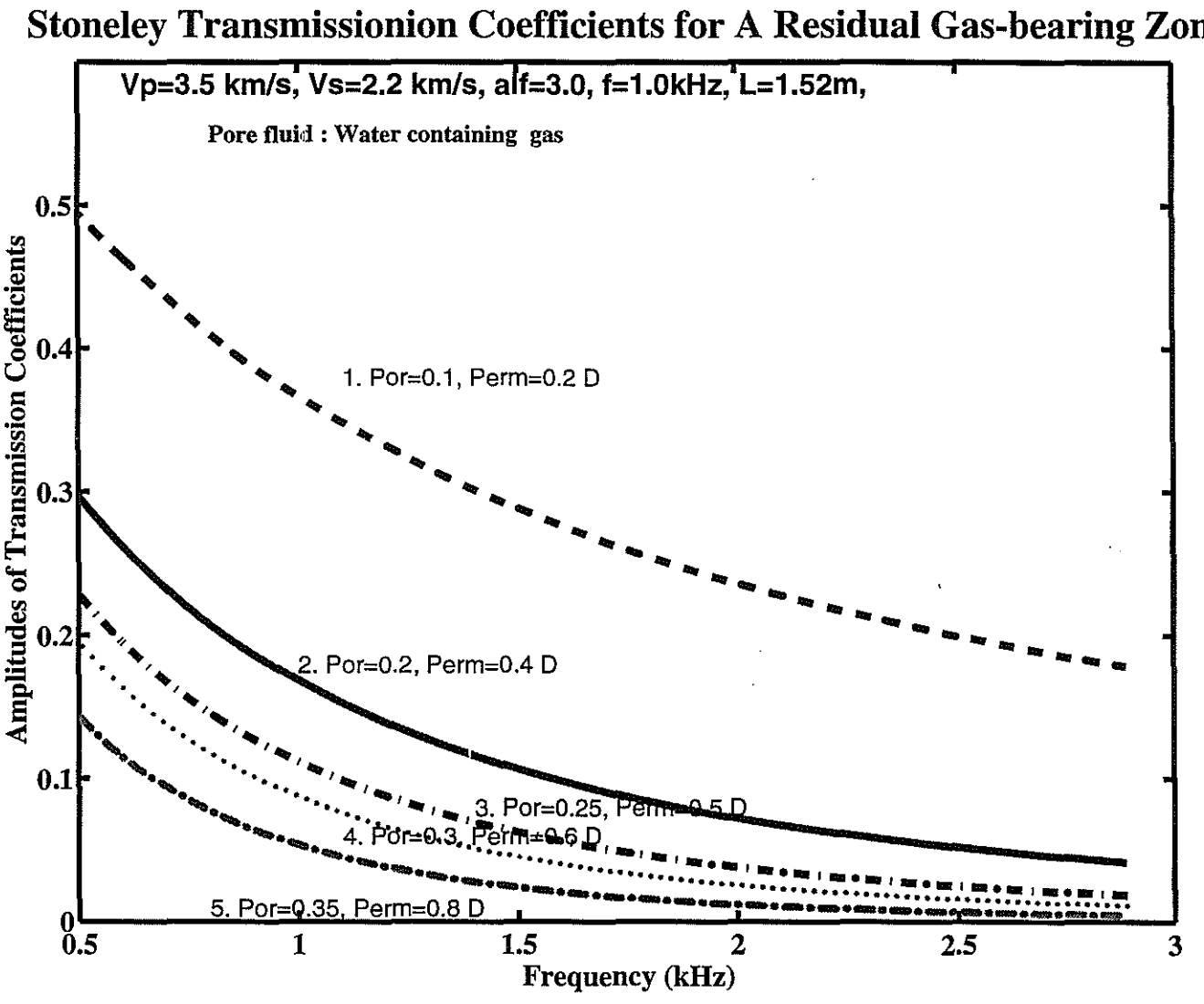

Figure 13b: Stoneley wave transmission and reflection coefficients for a residual gas-bearing zone. b. Transmission coefficients.

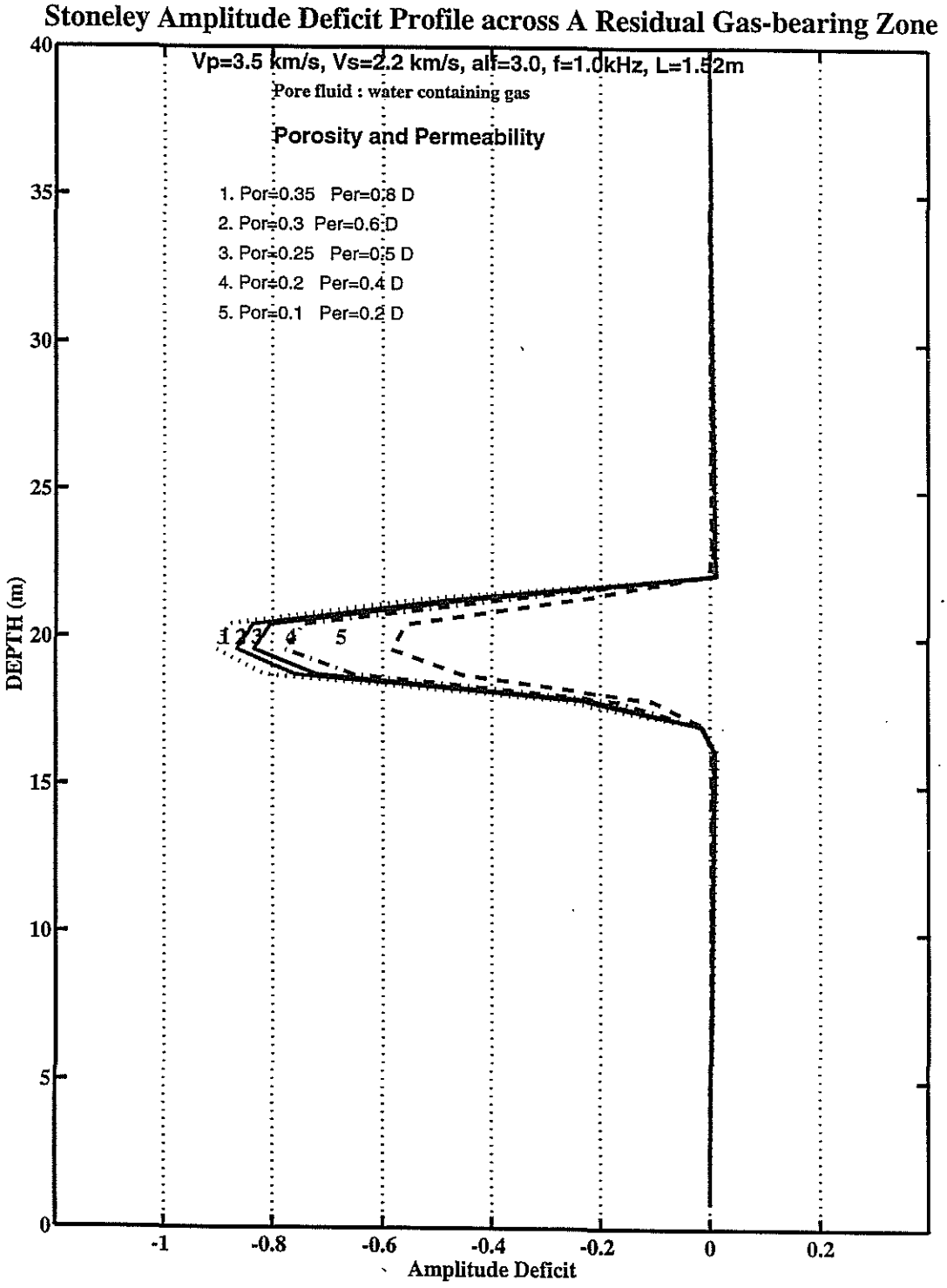

Figure 14: Stoneley wave amplitude deficit profiles across a residual gas-bearing zone with different porosities.

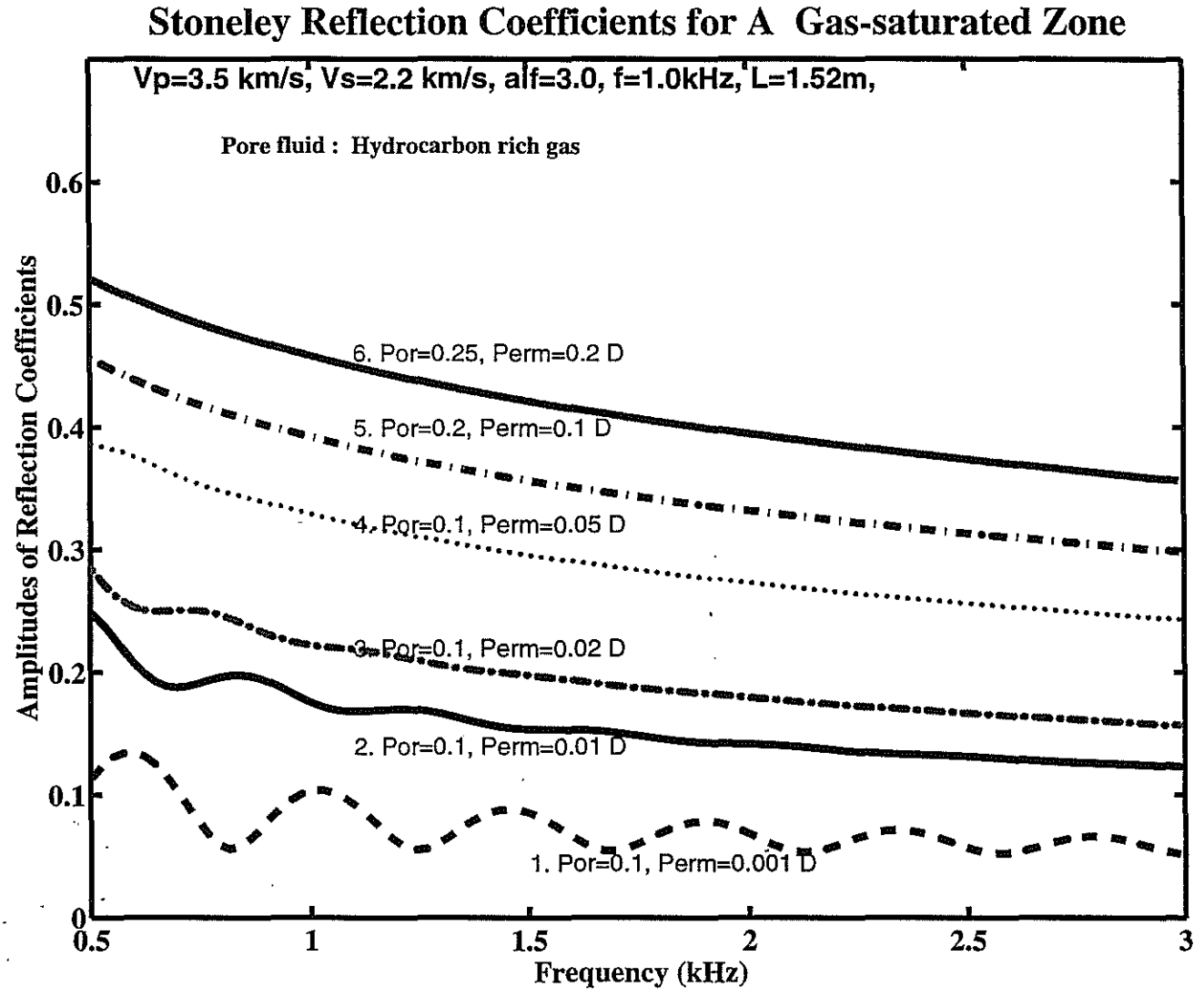

Figure 15: Stoneley wave reflection coefficients for a fully gas-saturated zone. 1. Permeability is 0.1 Darcy. 2. Permeability is 50 milliDarcy. 3. Permeability is 20 milliDarcy. 4. Permeability is 5 milliDarcy. 5. Permeability is 1 milliDarcy.

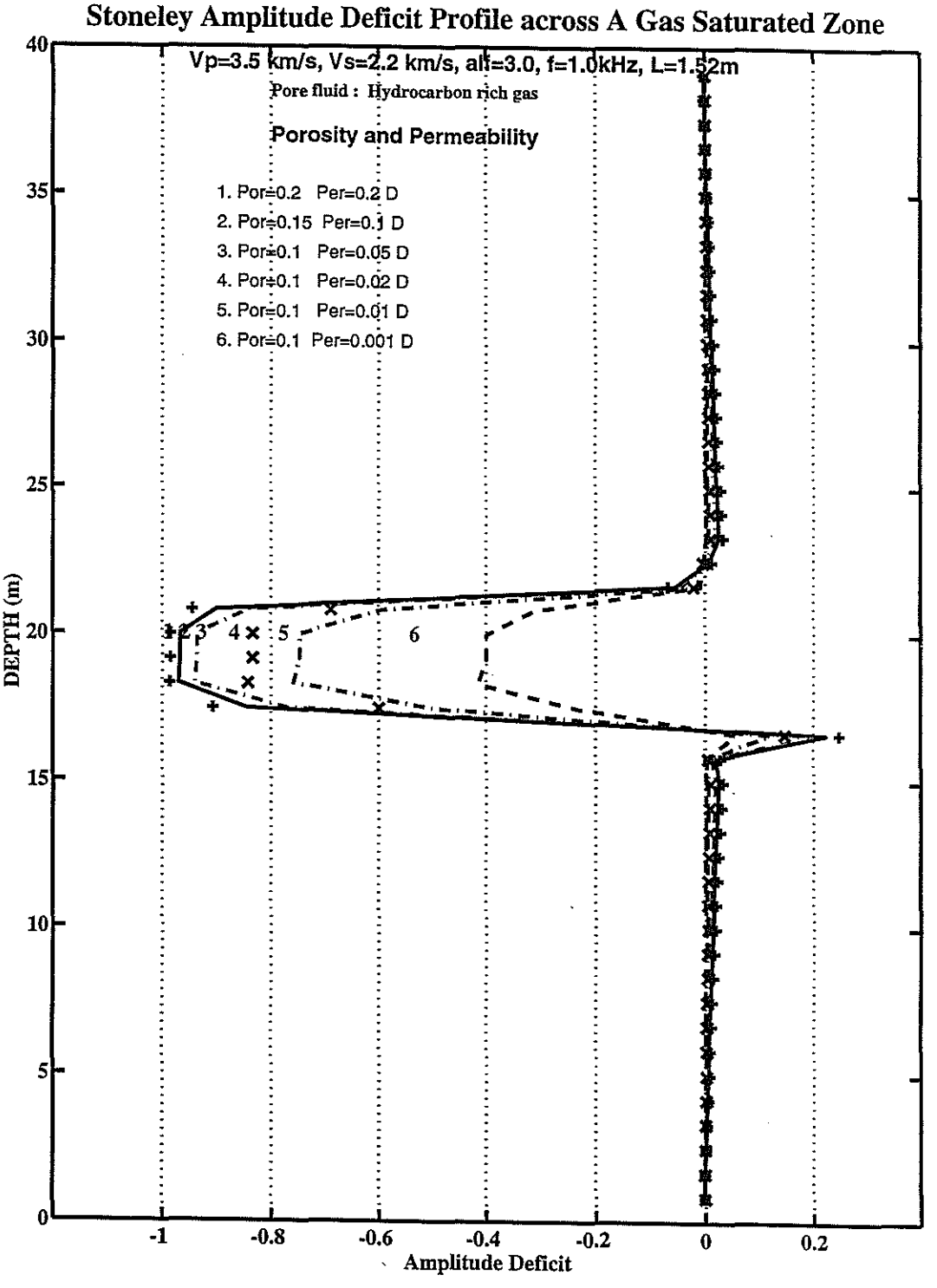

Figure 16: Stoneley wave amplitude deficit profiles across a fully gas-saturated zone with different permeabilities.

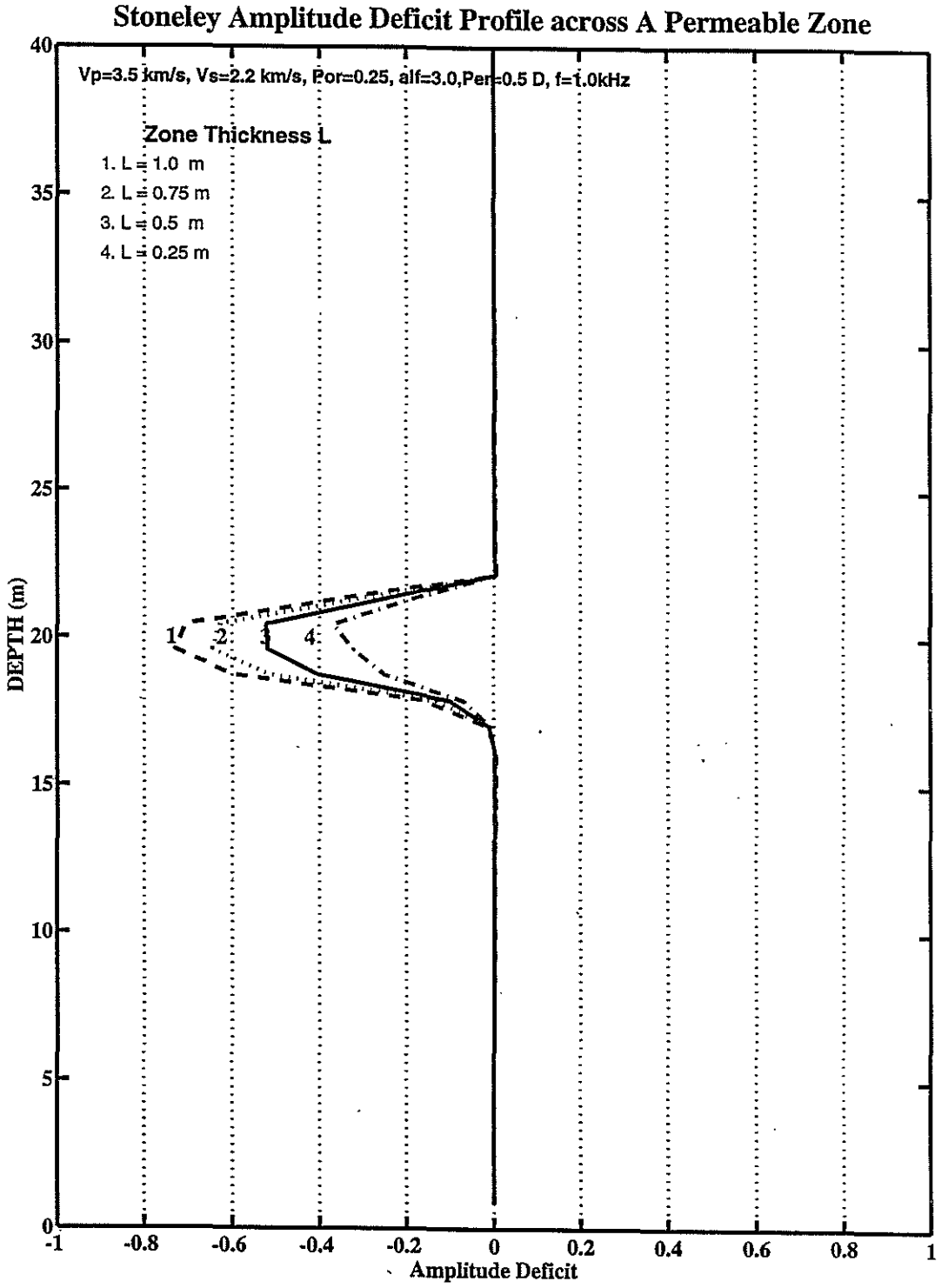

Figure 17: Stoneley wave amplitude deficit profiles across a residual gas-bearing zone of different thickness.

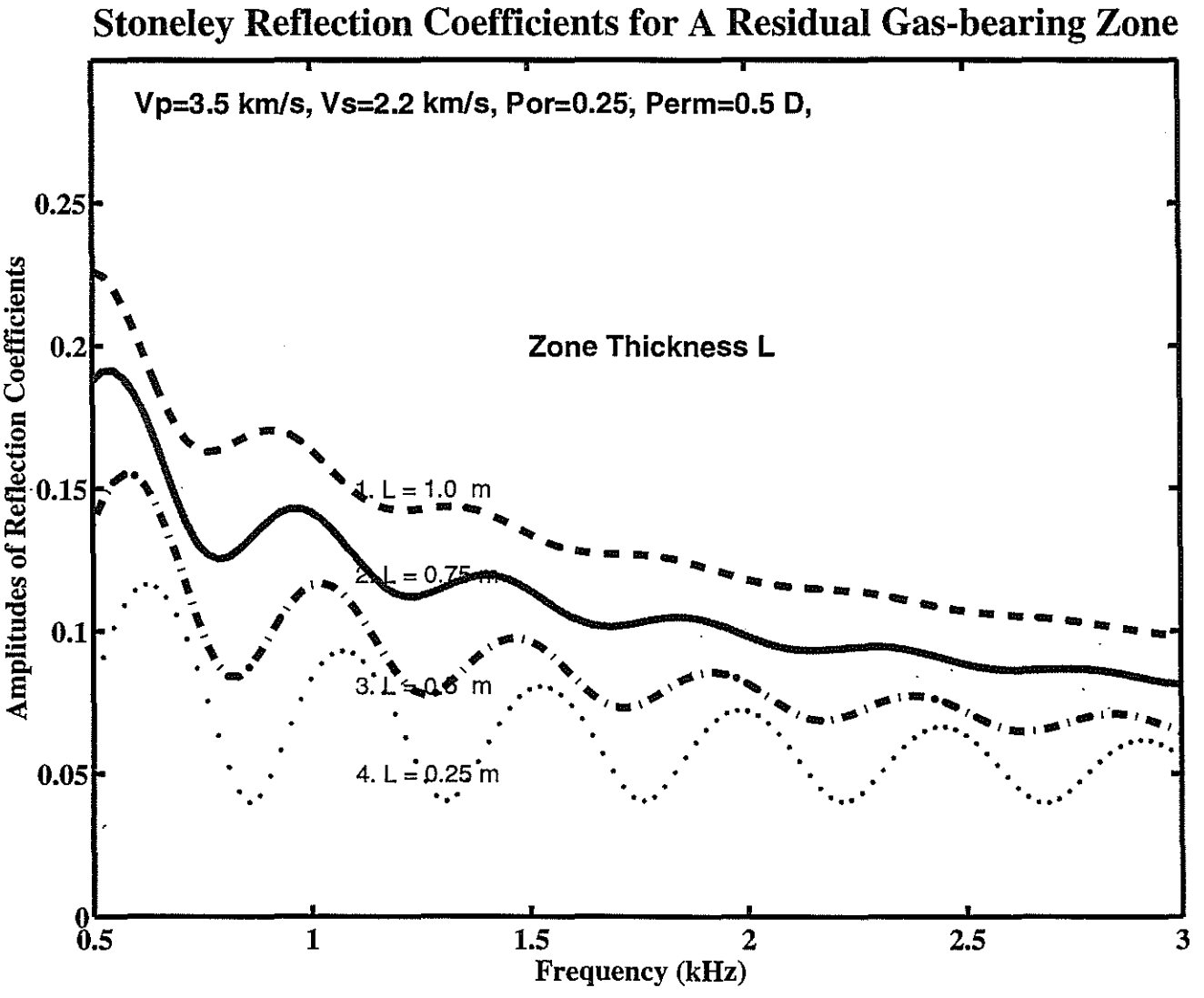

Figure 18: Stoneley wave reflection coefficients for a residual gas-bearing zone of different thickness.